HAROLD

Version 4.3.1

CONTENTS

CONTENTS

CONTENTS

Chapter

1

Introduction

This is a Windows version of Harold.

HAROLD is a computer program designed to simulate the electrical, optical and thermal characteristics of Fabry-Perot laser diodes, based on well-established physical models. For a given layer structure and material properties it yields a large amount of simulation data describing the lasing characteristics. When combined with the appropriate mechanisms and parameters, it may become a helpful design tool either to optimize existing lasers or to assess new designs.

This version of HAROLD implements the longitudinal dimension (cavity axis) in the solution of the device equations, which are now solved in a 2-dimensional mesh. The user is allowed to change from isothermal to self-heating operation, as well as to choose a 1D (vertical) or full 2D simulation mode, by means of appropriate switches.

In addition, several improvements have been made, resulting in a better overall performance.

1.1 Installation

Please refer to the Installation Guide to install your product.

1.2 Changes Log

Version 4.3.1

- Added adaptive bias step size feature to help avoid convergence problems resulting from the use of too large a voltage increment or current step

- Improved voltage to current-bias switching

- Added feature to allow residuals/normalised corrections to be displayed in message log as simulation is running

- Maximum residual/normalised correction now used as convergence criteria instead of average values

- Fixed bug in waveguide mode solver

- Added scripting menu items

Version 4.3

- Now the user can specify the names of the alloy compositions (x, y) and their function dependence.

- Removed user-defined quantum well escape time /capture time ratio introduced in 4.2.4 and replaced it with a more accurate model, which calculates the ratio by taking the population of higher levels into consideration .

- The mobility now supports temperature dependence.

- Now has a parallel and perpendicular effective mass in material - engine uses appropriate automatically.

- Added strain in barriers.

- Fixed export of Auger rate in PicWave-Link - was too low.

- Implemented TM mode finder (before was using TE mode for both polarisations).

- Can now consider electron/hole wavefunction overlaps.

- Fixed bug in 1D drift/diffusion solution finder that was sometimes causing convergence problems.

- Added feature to iterate a voltage drive until one reaches a certain current – allows a more evenly spaced current interval.

- Improved waveguide mode solver to ensure it finds mode with largest confinement rather than just first mode – avoids problems with e.g. high-index contact layers.

Version 4.2.8

- Now supports installation on 64-bit OS's.

Version 4.2.7

- Minor changes to improve 2D run-mode

Version 4.2.5

- Cosmetic changes to PicWave link and fix of AIR export

Version 4.2.4

- Added gain-spectrum export file and a plot showing all gain-spectra

- Many minor improvements to the PicWave link interface

Version 4.2.4

- Added quantum well escape time /capture time ratio (previously assumed to be 1.0).

- Removed many static array limits. Added more error checks.

Version 4.2.3

- Fixed convergence problem at transition between low and normal voltages.

Version 4.2.2

- PicWave -Link: added MXPARM MYPARM to .mat file.

Version 4.2.0

- Improved Shroedinger solver - replaced with more robust version which solves e.g. near-decoupled and fully decoupled quantum wells automatically.

Version 4.1.0

- Implemented link to Photon Design's time domain laser model PicWave – export PicWave -compatible gain model, recombination rates, refractive indices and other

material parameters to permit advanced device modelling in PicWave while taking detailed account of the quantum well structure using Harold.

Chapter

2

Learning Harold

2.1   A 1D Example

In this section we outline how HAROLD can model certain key design parameters of an AlGaAs laser. A more formal development of HAROLD can be found in subsequent chapters.

➢ Start HAROLD. The main window will appear

➢ From the **File** menu select **Open Project** or press the ⛁ button.

➢ From the Harold\examples subdirectory, select **example1.hpj** and press Enter or click Open.

The **example1.hpj** project will be opened. It contains the following items:

HAROLD device (cavity1)

HAROLD epitaxial layer structure (layers1)

HAROLD simulator (sim1)

Two *HAROLD trap definition sets* (trap7, trap7qw)

Quantum well definition set (qwlevels1)

➢ Double-click on the ▦ icon. This will display a panel that can be used to edit the epitaxial layer structure of the laser. This panel is shown in **Figure 2.0**.

The panel displays a list of layers. If you click on each line of the list, you will observe the parameters in the panel changing reflecting the material
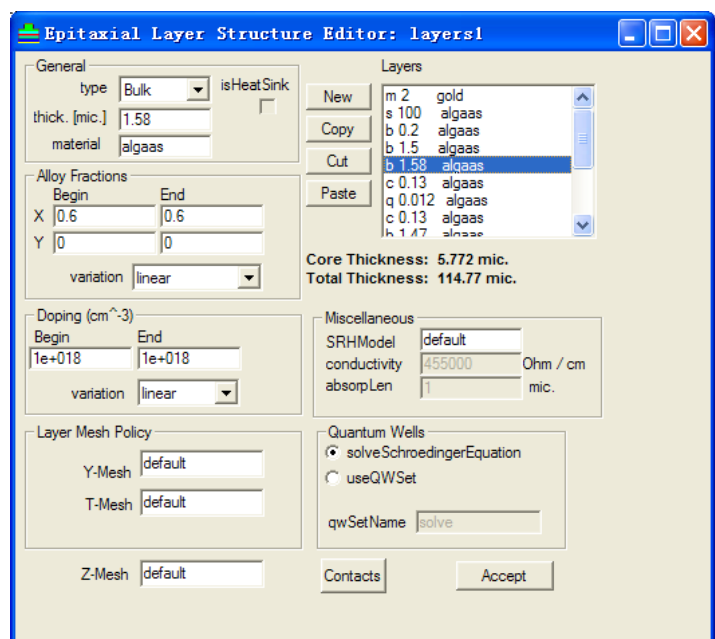
Figure 2.0: The *Epitaxial Layer Structure Editor* panel   for the AlGaAs laser structure in example1.hpj.

type, thickness, material, alloy variation, etc. of the currently selected layer.

As can be seen, a two-micron thick layer of gold is represented in the list as:

"m 2 gold"

where 'm' stands for *metal*. Other types of layer include *bulk* ('b'), *substrate* ('s'), *confinement* ('c') and *quantum well* ('q'). This device therefore corresponds to an AlGaAs laser with a single quantum well layer, with two gold contacts and a copper heatsink.

Also on this panel, the core thickness and the total thickness is given. The core of the device is defined as the collection of layers that are not metal layers or substrate layers. See chapter 5 – the graphical user interface reference for more details.

➤ Now, on the main window of HAROLD, click on the ![icon] icon.

This will bring up a panel that will describe the properties of the laser cavity. Here you can alter basic properties such as the length and width of the laser cavity or you can alter more advanced properties such as the reflectivity of the facet mirrors, the Schockley-Read Hall electron lifetime, etc. **Figure 2.1** shows the device properties panel. As can be seen, this is a 600-micron long, 100-micron wide laser where both of the mirrors have a reflectivity of 95%.

Notice also that the "**Layers**" property has been set to layers1, which is the name of the epitaxial layer structure node that we viewed earlier. Thus this laser uses the layers1 epitaxial structure. In principle you can define several epitaxial layer structures in one project and for

Figure 2.1: The device properties panel for the example1.hpj laser structure.

the same laser cavity, just "swap-in" the layer structure you wish to model.

➤ After you have inspected any parameters you wish to see, click on the ![icon] icon on the main window of HAROLD.

This will bring up a HAROLD simulator panel. This is shown in **Figure 2.2**. The simulator has been set up to run a 1-dimensional self-consistent, self-heating simulation of the laser cavity where the bias current is increased from 0Amps to 0.8Amps in steps of 0.1Amps. After the simulation, we will be able to observe functions of position within the core of the laser at the final current bias of 0.8 Amps. We will also be able to observe bias varying quantities such as the active region temperature.
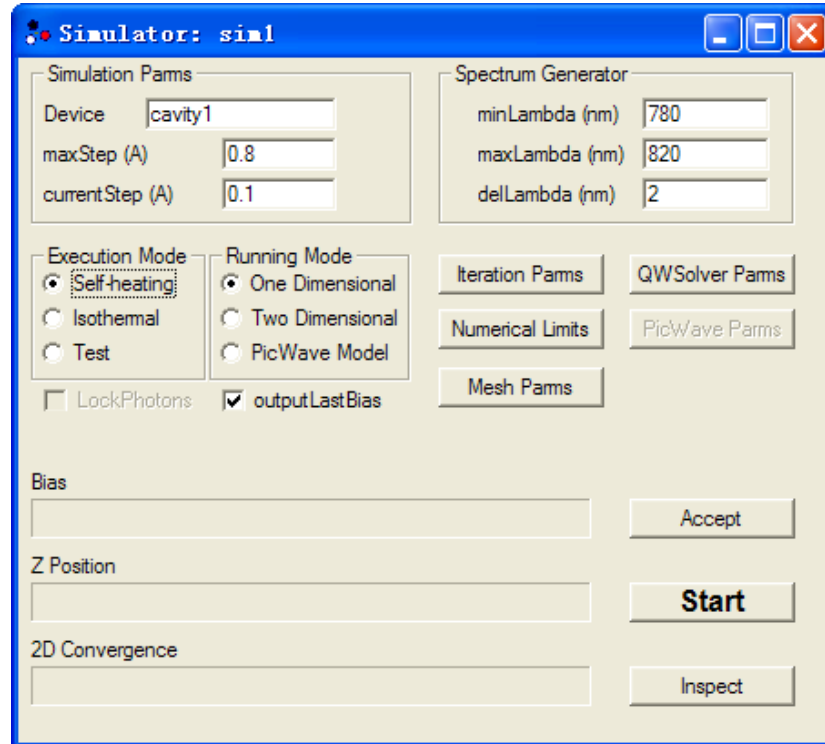
Figure 2.2: The Simulator panel for the example1.hpj laser structure.

➤ Press the Start button on the *Simulator* panel to start simulation. The label of the button will change to Stop which indicates that you can abort the simulation by press the button again.

➤ When the simulation has completed, the Stop button will change to Start again. Now press the Inspect button. This displays the HAROLD results dialog box. From here, all the results that have been obtained from the simulation can be visualised. (See chapter 5.4)

➤ Select the "*Per Bias Results*" tab. This will bring up a list of all available functions of current, voltage or current density.

➤ From the "Available plots" list, select "Optical Power (facet 2)" and press the Plot button next to this list. This will plot the optical power incident on the output facet (i.e. facet 2). **Figure 2.3** shows the resultant plot. As can be seen, this is a relatively
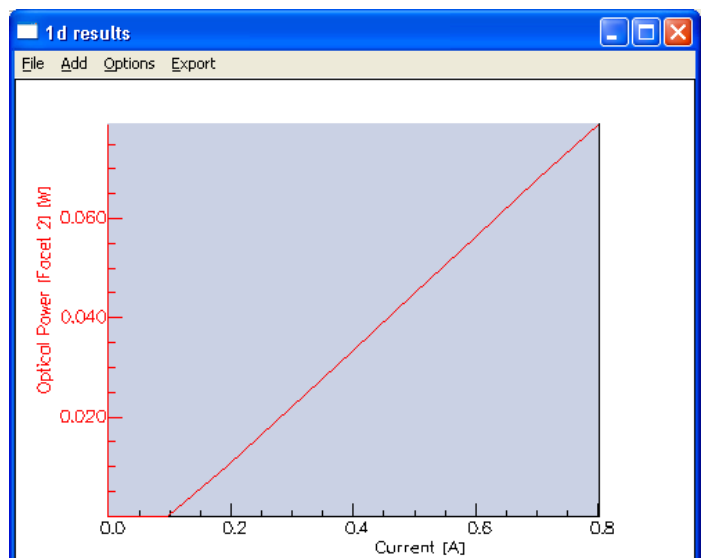
Figure 2.3: Graph of optical power incident on the right hand side facet as a function of the bias current.

high threshold laser (the threshold being ~100 mA). Beyond the threshold, the optical power is increasing almost linearly with increasing current.

HAROLD can also plot quantities that are a function of the core position. It can also plot more than one function at a time.

➢ On the results dialog box, select the "*1D Results*" tab.

➢ In the "Available Plots" list, select "Conduction Band".

➢ Now press the ==> button. This will move "Conduction Band" into the "Multiple plots" list.

➢ In the "Available Plots" list, select "Valence Band".

➢ Once again, press the ==> button to move "Valence Band" into the "Multiple plots" list.

➢ Set npoints to 1000.

➢ Press Plot next to the "Multiple plots" list. Two lines will appear, one red and one green corresponding to the conduction and the valence bands, respectively.

➢ On the plot window, select Options/Axes. On the options dialog that appears, check the "plot all on same y-axis" option and press OK. Now the graphs will be drawn on the same axis, which makes the results a lot clearer. Figure 2.4 shows the resultant plot.
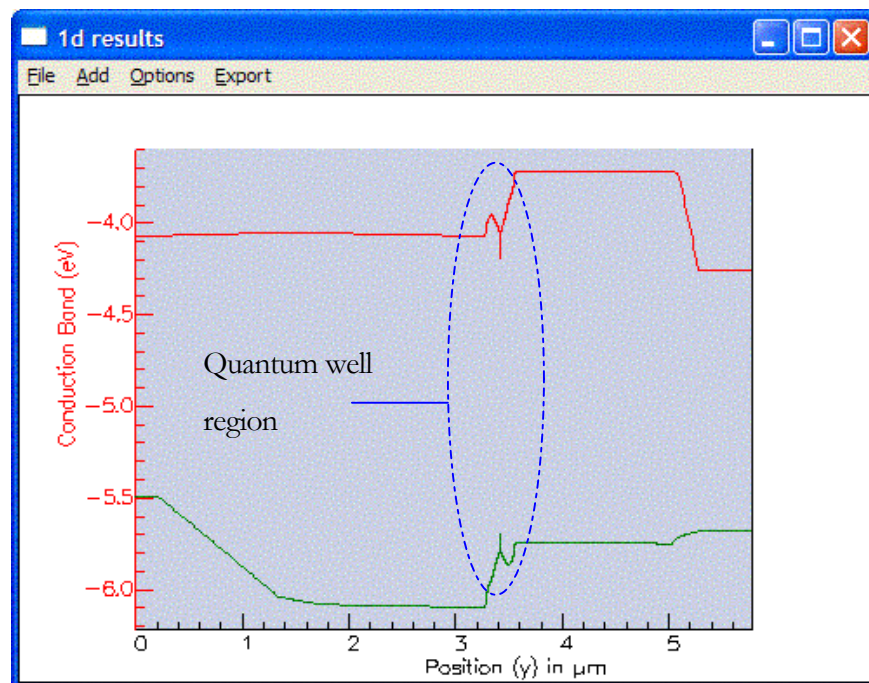
Figure 2.4: The conduction and valence band energies vs core position showing clearly the position of the quantum well. Notice the dip in the conduction band and the slight rise in the valence band near the uppermost contact. This causes a high density of charge carriers at this point. It is most likely that this would cause a degrading of the performance of the laser diode since this will increase the transit time for carriers entering the quantum well.

Now we shall observe the effect of increasing the series thermal resistance at the upper boundary of the device.

➤ Close the results dialog down and select the device properties panel again.

➤ Press Heat Sink . This will display a dialog box where you can alter the properties of the heat sinks. This is shown in figure 2.5.

cavity1: Heatsink Properties

Parameter	Value	Units
U-Temp	25	C
U-ThermResist.	0	C cm^2 W^-1
U-SeriesThermRes	80	C W^-1
L-Temp.	25	C
L-ThermResist.	0	C cm^2 W^-1
L-SeriesThermRes	1e+040	C W^-1

Figure 2.5: The heatsink properties editor. The yellow 'tool tip' box appears if you move the cursor over cells in the left-hand 'parameter' column. This is true for all the grid-like editors that can be found in HAROLD.

➤ Alter the series thermal resistance of the upper heatsink to 80 deg. C per Watt (as shown in **Figure 2.5**).

➤ Close the dialog down.

➤ Select the simulation panel and press "Start" to start the simulation.

➤ After the simulation has completed, press Inspect .

➤ On the results panel, select the *Per Bias Results* tab. From the available plots list, select "optical power (facet 2)" and press the plot button by the list. **Figure 2.6** shows the resultant plot. As can be seen the increased thermal resistance means that a greater proportion of the bias current contributes to the self-heating of the device. This results in a reduced dP/dI (c.f. **Figure 2.3**), where P is the optical power (facet 2) and I is the bias current, which continues to decrease as the current, and therefore the temperature, increases. This would eventually cause the device to stop lasing.
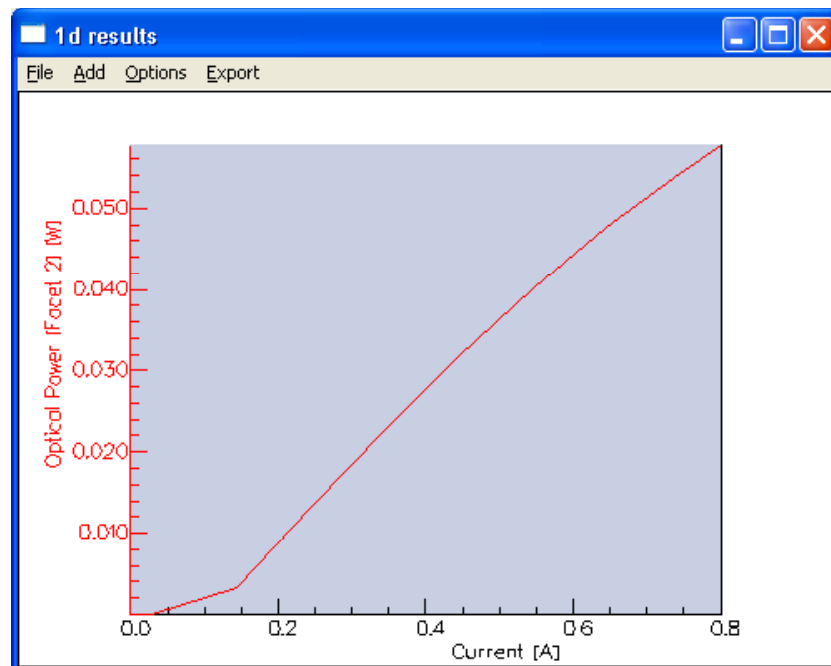
Figure 2.6: The optical power incident on facet 2 with an increased upper series thermal resistance.

2.2 A 2D Example

In this section we perform a 2D simulation of the same 808nm emitting AlGaAs laser modelled above. Using HAROLD we will model facet heating due to optical absorption and surface recombination.

➢ From the **File** menu, select **Open Project** or press the 📇 button.

➢ From the Harold\examples subdirectory, select **example2.hpj** and press Enter or click Open.

The example1 project will be opened. It contains the following items:

HAROLD epitaxial layer structure (layers)

Quantum well definition set (gmp81qw)

Two *HAROLD trap definition sets* (trap7, trap7qw)

HAROLD simulator (Simulator)

HAROLD device (cavity1,2,3)

➢ Double-click on the 📍 icon. This will display the Simulator
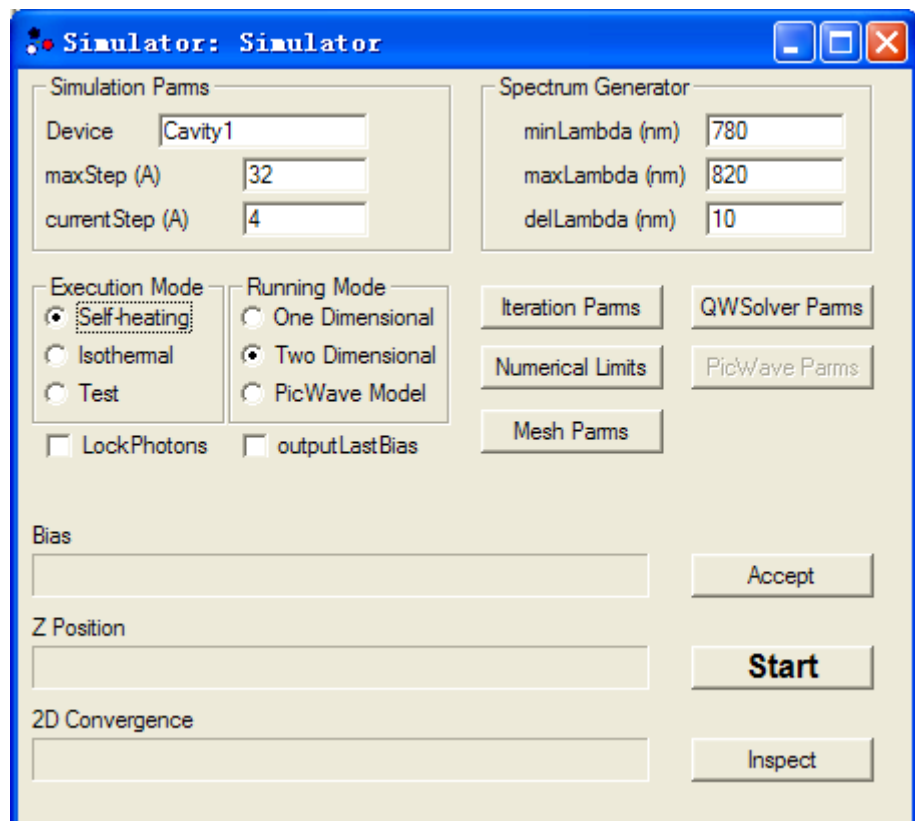
2.2.1 Without Heating Effects

We are first going to model this laser without any facet heating effects.

➢ Click on the *Two Dimensional* radio button and click Start .

HAROLD will perform a two dimensional simulation. This will take approximately fifteen minutes.

➢ Once this is finished, click on the Inspect button, this brings up the Simulation results panel.

➢ Click on the *Per Bias Results* tab, highlight "Optical Power facet 2", and click on the arrow button to bring this selection into the Multiple plots box.

➢ Repeat this procedure for "Active Region Temperature"
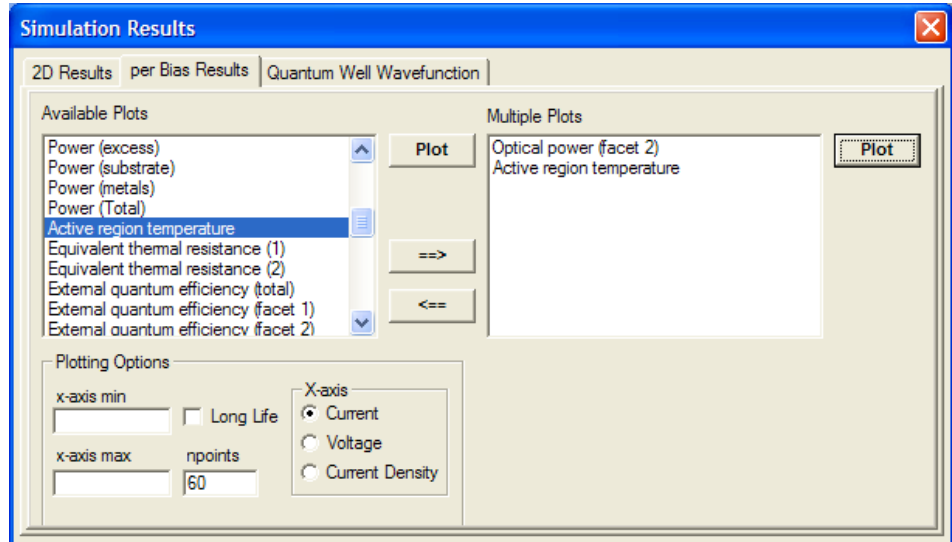
➢ Click Plot on the right of the Multiple Plots box.
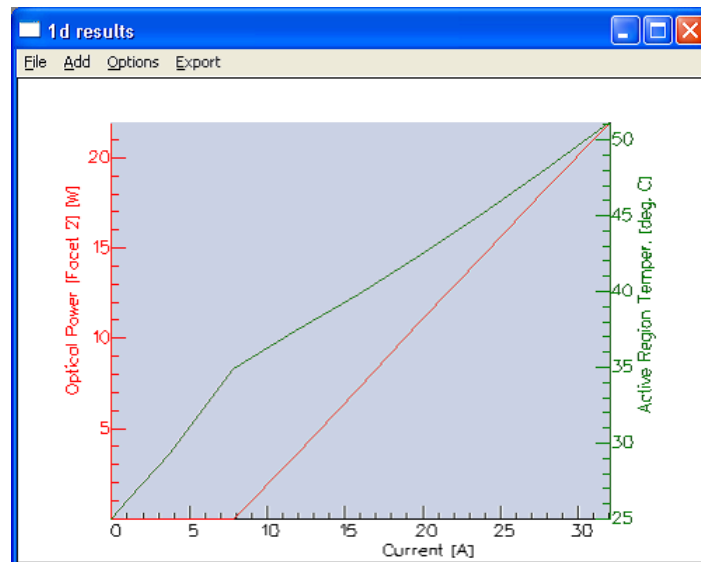
This is a plot of the optical power (left axis), and the quantum well temperature (right axis) as a function of the input bias. Notice that the lasing threshold is around 6A. (This current is quite large due to the fact that the laser itself is 4000um wide)

➢ Remove the two plots from the Per Bias Tab by highlighting them and using the arrow button.

➢ Move the following four plots into the Multiple Plot box:

- Power (Joule)

- Power (nonradiative recombination)

- Power (free carrier absorption)

- Power (excess)

➢ Click Plot on the right of the Multiple Plots box.

➢ From the Options menu of the Graph, select **Axes/Plot** all on same axis
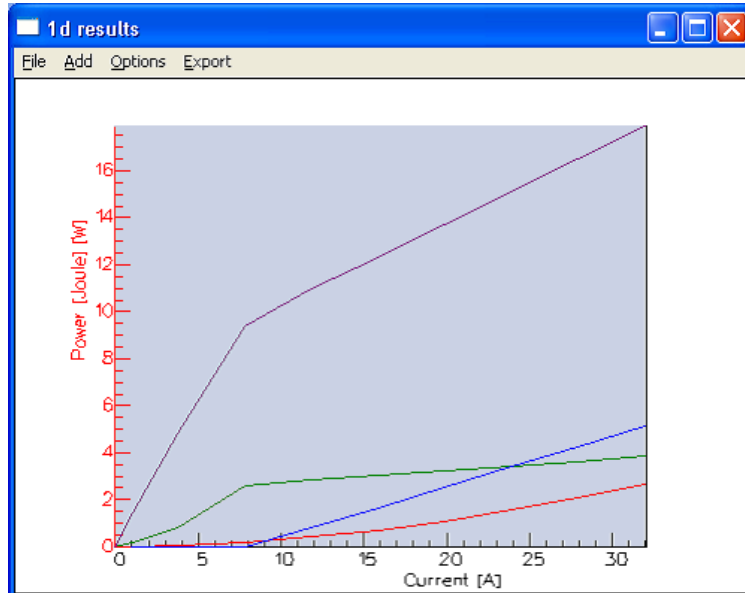
This graph shows the contribution of different heating mechanisms as a function of the injected input bias.

Power (Joule), Power (nonradiative recombination), Power (free carrier absorption) and Power (excess) are given by the equations (3-72)-(3-75) respectively. Notice here that the main contributor to the heating mechanisms is the excess power – this value represents all remaining power dissipation mechanisms. Also, note that the scattered optical power at the mirror facets is included within the excess power. See Chapter 3.15.1 for more information.

➢ On the *Simulation Results Panel* select *2D Results/Thermal/Temperature*

➢ Set nz = 600 and click Plot
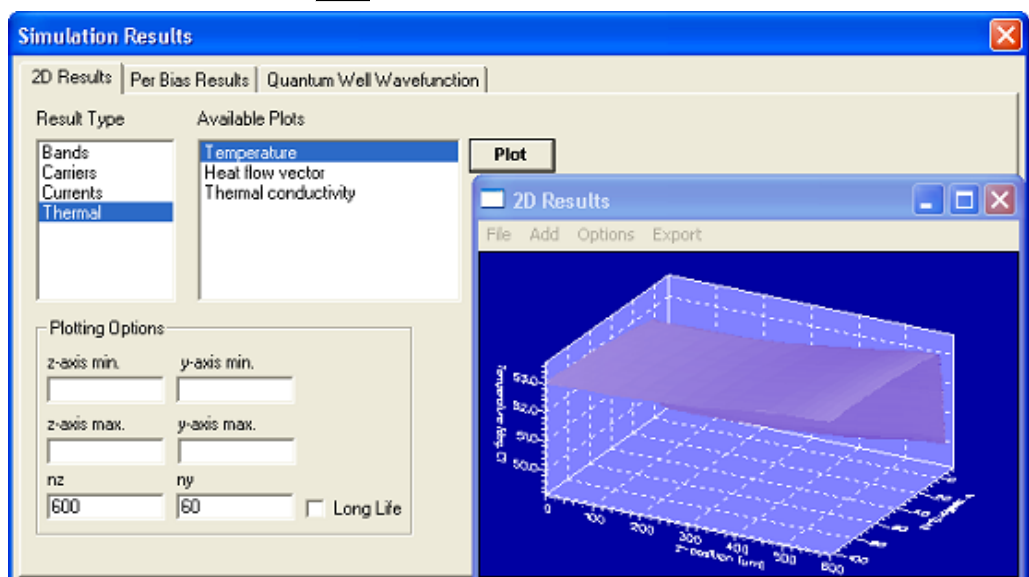
The resulting plot is a 2D surface plot displaying the temperature in the cavity. Notice that the increase along the cavity is only gradual. At Z = 600, the temperature is around 54 degrees, when we later introduce facet heating due to optical absorption this will rise sharply.

➢ Right-Click on the **2D Plot/Plot Cross Section.**

➢ Select vertical section, at Z =300 (the centre of the device)

➢ From the 1D plot select **Options/Axes**, and re-scale the x-axis from +/-10um
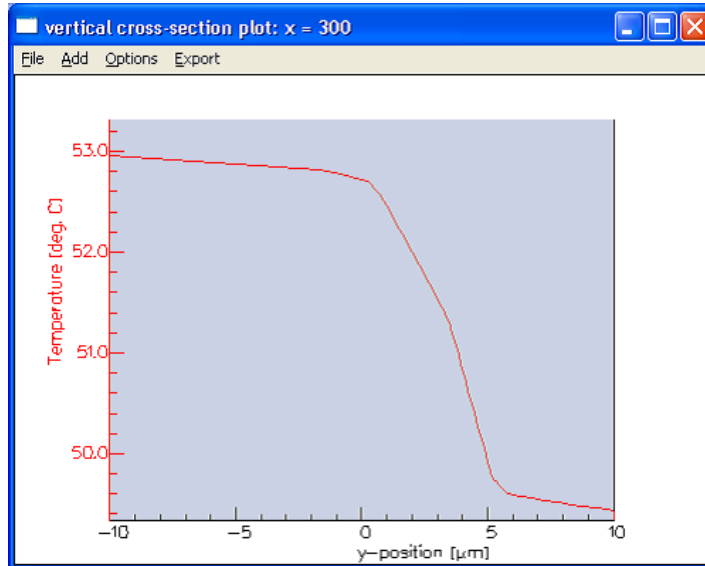
This shows the temperature cross-section (at I = 32A) along the centre of the cavity. Note that the quantum Well is centred on 3.416um.

Similarly for Z=600, the temperature cross-section is as below. The plot is very similar to that at Z = 300. I.e. there is no sharp rise in temperature at the facet.
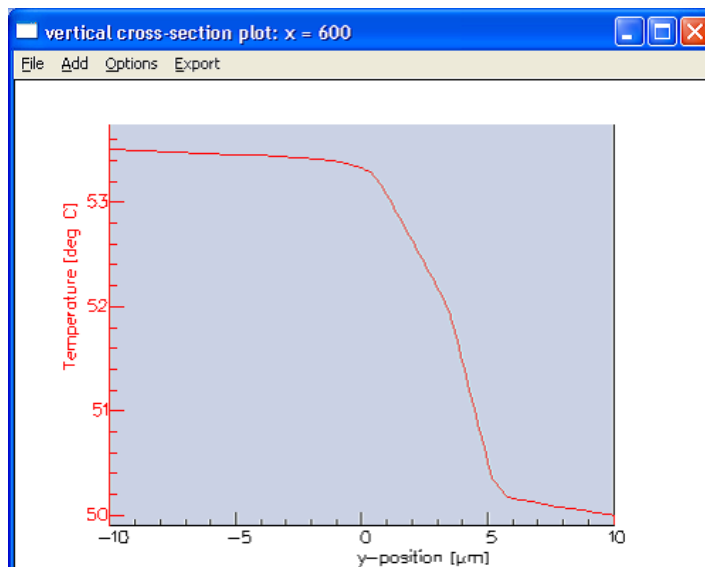
2.2.2 Heating Due To Optical Absorption

Now we will study the heating effect due to optical absorption at the right hand side facet. To do this all we have to do is set an absorption coefficient the right mirror. This is done on the Device Panel. This has already been done for you in Cavity2.

➢ From the main window of HAROLD, double click on the *Device* Node "Cavity2" in the project tree.
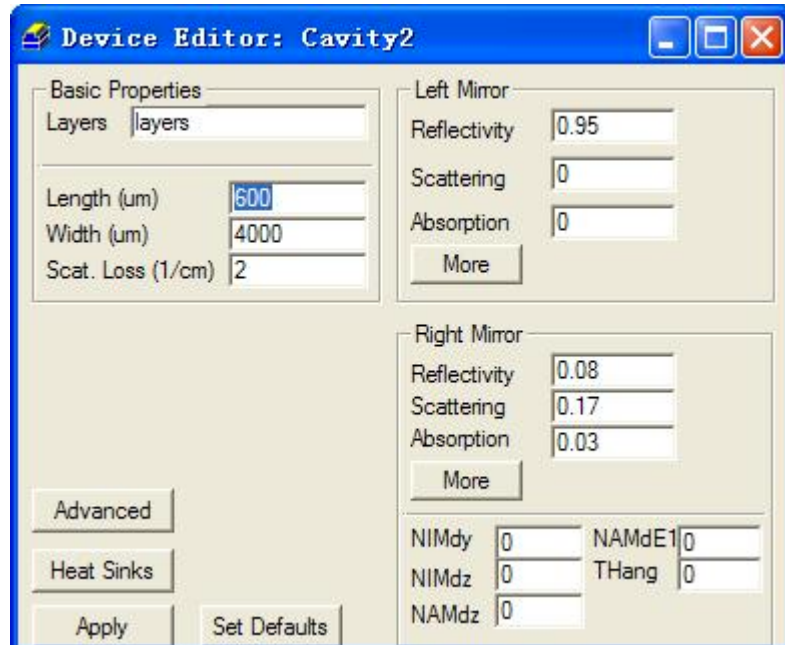
➢ Notice that in the **Right Mirror** box there is an absorption of 0.03 (3%)

➢ Open the Simulator again.

➢ In the *Simulation Parms* box change the *Device* name to *Cavity2*

➢ Click Start

➢ Once this has finished, click on Inspect.

➢ Select *2D Results/Thermal/Temperature*

➢ Set nz = 600 and click Plot

2-13
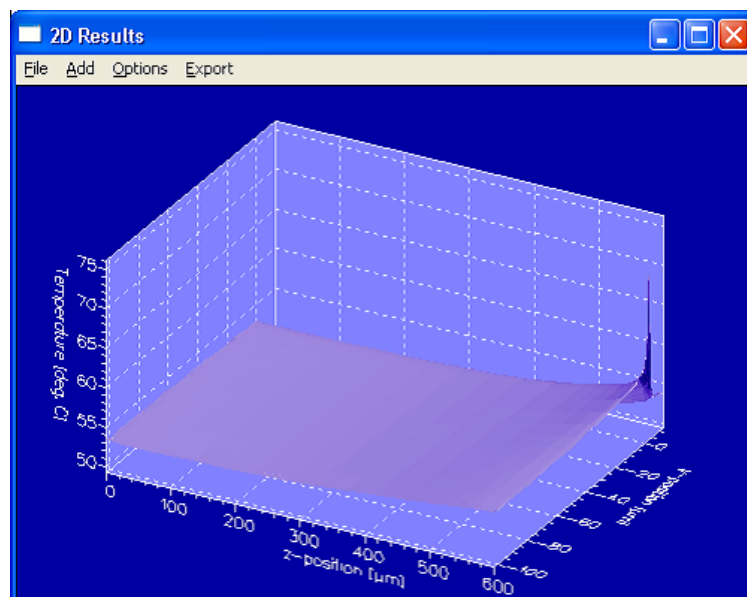
Notice that there is now a large increase in temperature at the mirror. This is due to the 3% absorption. The peak (obviously) occurs in the active region centred on x=3.416

➢ Right-Click on the **2D Plot/Plot Cross Section**.

➢ Select horizontal section at x = 3.416 (the centre of the active region) – this will plot the temperature in the active region as a function of Z.
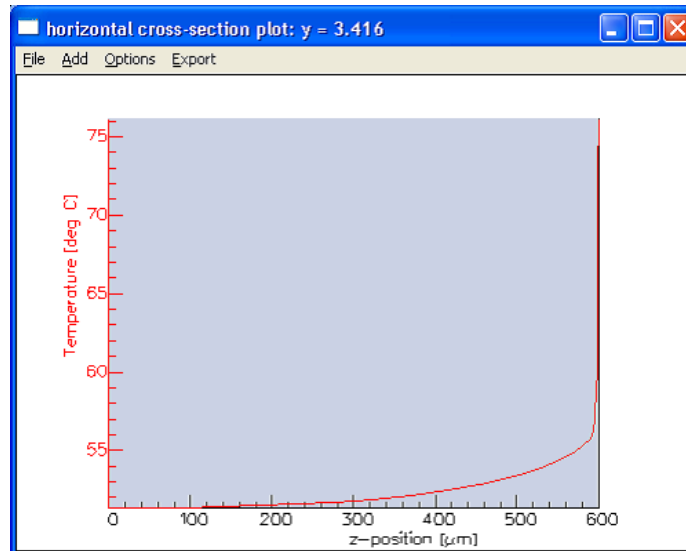
Notice that now there is a sharp rise in temperature close to the mirror. If, as before, we plot the vertical cross-sections at Z=300um (left below), and Z=600um (right below) we see this more clearly. (Again the active region is centred on 3.416um)
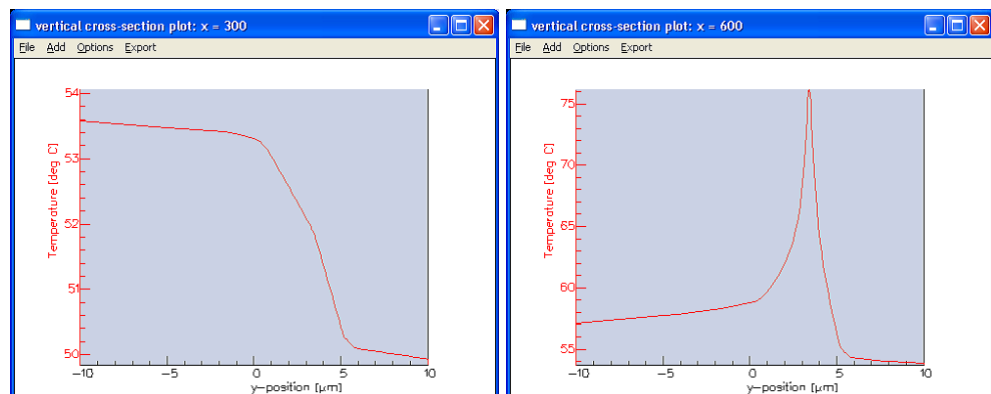
➢ If you wish, you may set the optical absorption of the mirror to be 9% and re-do this simulation. You would obtain the results given in the diagrams below.
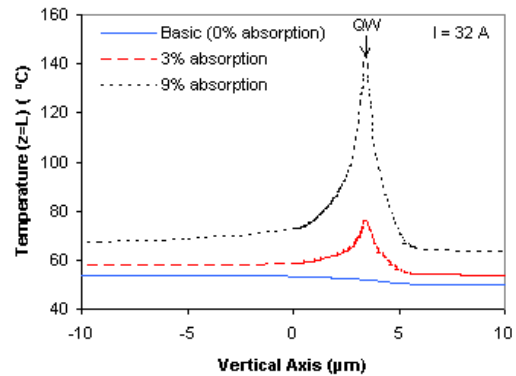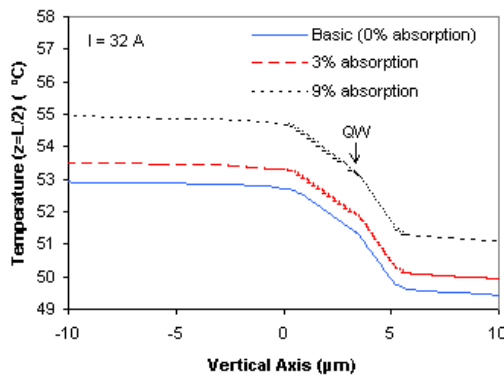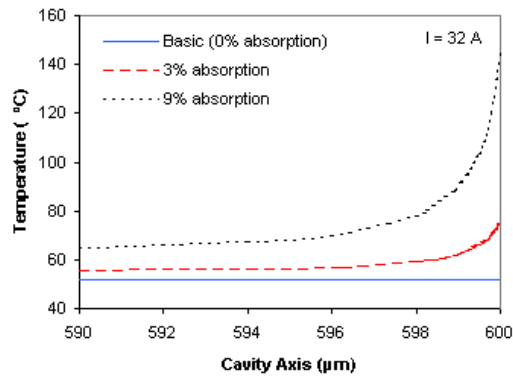
2.2.3 Heating Due To Surface Recombination

We can also model the mirror heating due to surface recombination.

➢ From the main window of HAROLD, double click on the Device Node "Cavity3" in the project tree. Notice that the right mirror absorption is now set to zero, as it was in Cavity1

➢ Select RightMirror/More

Notice that a surface trap density of 5x10^17 has been set here to model heating due to surface recombination.

➢ Open the Simulator again.

➢ In the *Simulation Parms* box change the **Device** to *Cavity3*

➢ Change the **maxCurrent** = 20 (Amps)

➢ Click Start

➢ Once this has finished, click on the Inspect Button.

➢ Select *2D Results/Thermal/Temperature*

➢ Click Plot
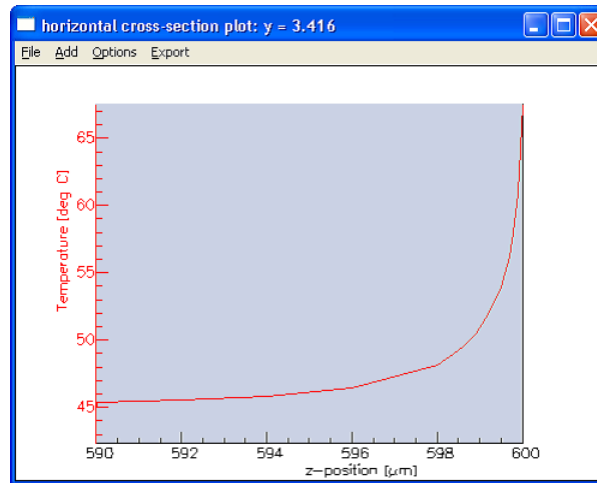
Notice that due to the surface recombination, there is a sharp rise in temperature close to the mirror.

If you perform this simulation, again for 40, and 60 Amps you will be able to reproduce the graph seen below.

Chapter

3

The Model
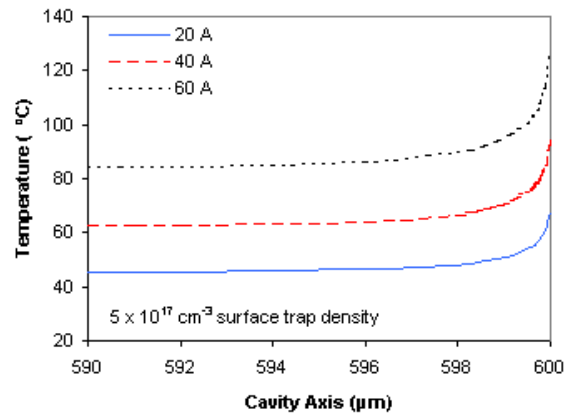
3.1   What is HAROLD capable of doing?

HAROLD solves the appropriate differential equations in the vertical and longitudinal direction, for a quantum well laser with arbitrary structure and composition. Both single and multiple quantum well lasers can be modelled. A state of the art capture/escape model for carriers in a quantum well is implemented. Both pulsed (isothermal) and CW (self-heating) operation conditions can be simulated. Materials include ternary and quaternary alloys. Among the data that HAROLD is able to generate, one can obtain:

- Light versus current characteristics

- Electrical/thermal characteristics

- Electrostatic potential, electric field and current distributions

- Distribution of electron and hole concentrations, for both confined and unconfined carriers

- Bands and quasi-Fermi energies

- Quantum well sub-band with parabolic bands

- 2-d optical field distribution

- Local optical gain

- Gain and spontaneous emission spectra

- Lasing wavelength and output power

- Temperature and heat flow distributions

3.2   Philosophy of HAROLD

HAROLD is a two-dimensional simulator which solves, self-consistently, the Poisson equation, the current continuity equations, the capture/escape balance equations, the photon rate equation, and the heat flow equation. In addition, it solves the vertical and longitudinal wave equation and Schrödinger's equation.

HAROLD consists of two modules: the 1D module and the 2D module. The 1D module serves to bias the device to the desired operating point. This solution is used as an initial guess for the 2D module, which seeks a self-consistent solution of the electrical, optical and thermal equations, considering lateral effects induced by surface recombination at the facets, optical absorption at the facets, and the non-uniformity of the optical field.

Note that in the 2D model, the LI curves are calculated in 1D, and only at the end of the LI curve calculation is the 2D model started – i.e. the 2D model computes for one bias point at a time. The facet absorption is taken into account by multiplying the output power at each facet by (1- absorption), but the secondary effect of facet heating on the LI curve is not taken into account. It is assumed that the facet heating is extremely local (2- 5 μm) in comparison with the typical longitudinal dimension of the device, and that therefore they are affecting very little the 1D LI.

The respective flow charts for the 1D and 2D modules are shown in **Figure 3.1** and **Figure 3.2**.

3.2.1 Features

The following features are incorporated into HAROLD:

- **DEVICE STRUCTURE** HAROLD accepts arbitrary laser structures. Material parameters are introduced through material files, which allow user defined materials.

- **ELECTRICAL MODEL** Full vertical-longitudinal self-consistent solution of the electrical equations (Poisson, drift-diffusion and capture/escape) for both types of carrier.

- **THERMAL MODEL** Full vertical-longitudinal solution of the heat flow equation, including the substrate, the metal contacts and the heat sinks. Power dissipation is treated locally and includes Joule, non-radiative recombination, free carrier absorption, excess power distribution, mirror scattering and mirror absorption.

- **OPTICAL MODEL** Photon distribution is in accordance with the optical mode of the laser cavity. The total photon density is determined by considering the gain/loss balance in the full cavity.

- **CAPTURE/ESCAPE MODEL** In QW regions, thermal equilibrium between confined and unconfined carriers is not assumed but described by means of appropriate capture/escape balance equations.

- **QUATERNARY ALLOYS** Utilization of quaternary alloys is fully supported through the material database.

- **MESH** According to the user specifications, HAROLD generates two different rectangular meshes to solve the electrical/optical equations and the thermal equations.

- **OUTPUT** HAROLD uses Photon Design's in-house plotting engine, SciGraph to visualize the computed results.

- **GAIN MODEL** Material gain for quantum well lasers are computed as a function of the wavelength and carrier concentration, using a parabolic band approximation.

- **RECOMBINATION** Shockley-Read-Hall, Auger, stimulated and spontaneous recombination processes are included. Advanced features, such as arbitrary specification of deep trap levels, are allowed on a layer-per-layer basis.

- **SURFACE RECOMBINATION** Recombination at the facets is included via deep trap levels at the mirrors.

- **BANDGAP NARROWING** Carrier-induced bandgap narrowing is included.

- **QUANTUM WELL** For QW structures the program can either determine the energy levels by solving the Schrödinger's equation, or use defined quantum well set, with the effective masses defined on a level-by-level basis.

- **STRAIN** The effect of strain on the QW levels is included.

- **THERMAL OVERHANG** Heat-sink overhang is implemented.

- **NON-INJECTING MIRROR** Suppression of current injection at the mirrors is implemented.

- **NON-ABSORBING MIRROR** Photon absorption attenuation at the mirrors is implemented

3.2.2 Assumptions and limitations

- Band and sub-band structure calculated in the parabolic band approximation. If the effective mass is anisotropic, then the perpendicular effective mass will be used in the quantum well energy calculation and the parallel effective mass will be used for carrier density calculation. Non-parabolicity and band mixing effects on the material gain are not explicitly in the simulation. Nevertheless, they can be treated in an effective manner via an external file, in which both level energy and effective mass can be specified individually for each level in the C, LH, and HH bands, at every QW.

- The effect of strain is considered as variations in energy levels of the LH and HH subbands, without affecting the corresponding effective masses.

- The QW level structure is not altered during the simulation.

- Vertical distribution of the optical field determined by solving the waveguide equation in the passive vertical structure approximation, and kept fixed throughout the simulation.

- Longitudinal distribution of the optical field does not explicitly consider absorption effects near the facets.

- Solution of the photon balance equation in the 2D module is performed out of the main self-consistent loop (see figure 2.2). The program first seeks a solution of the electrical equations in 2D at fixed photon density, which yields the total gain/loss for the cavity. Next, a modified 1D procedure is executed, using the obtained gain/loss, to solve self consistently the photon balance equation with the electrical equations at the central point of the cavity. With the new value of the photon density the previous solution of the 2D electrical equations is corrected. The procedure is repeated until consistency is reached.

- The voltage yielded by the 1D module at the specified current is used to control the device during the solution of the 2D equations. As a consequence, the final current may not exactly match the user-specified current. Typical deviations are less than 2%.

- The stability of the electrical/optical/thermal 2D solution may be affected when the device is simulated at the following operating conditions: 1) slightly above threshold, 2) at the onset of thermal rollover.

Figure 3.1: Flowchart of the one-dimensional module.
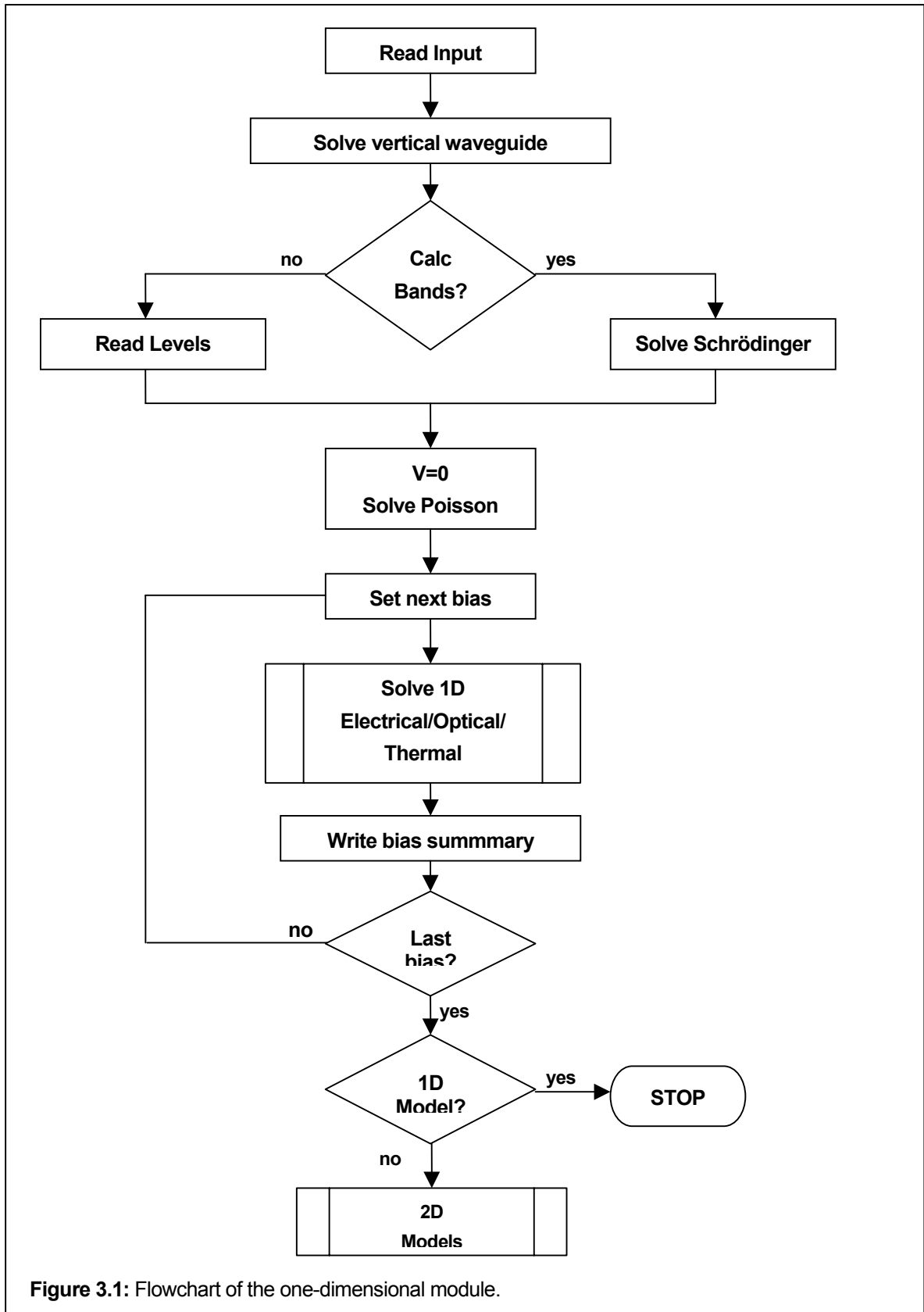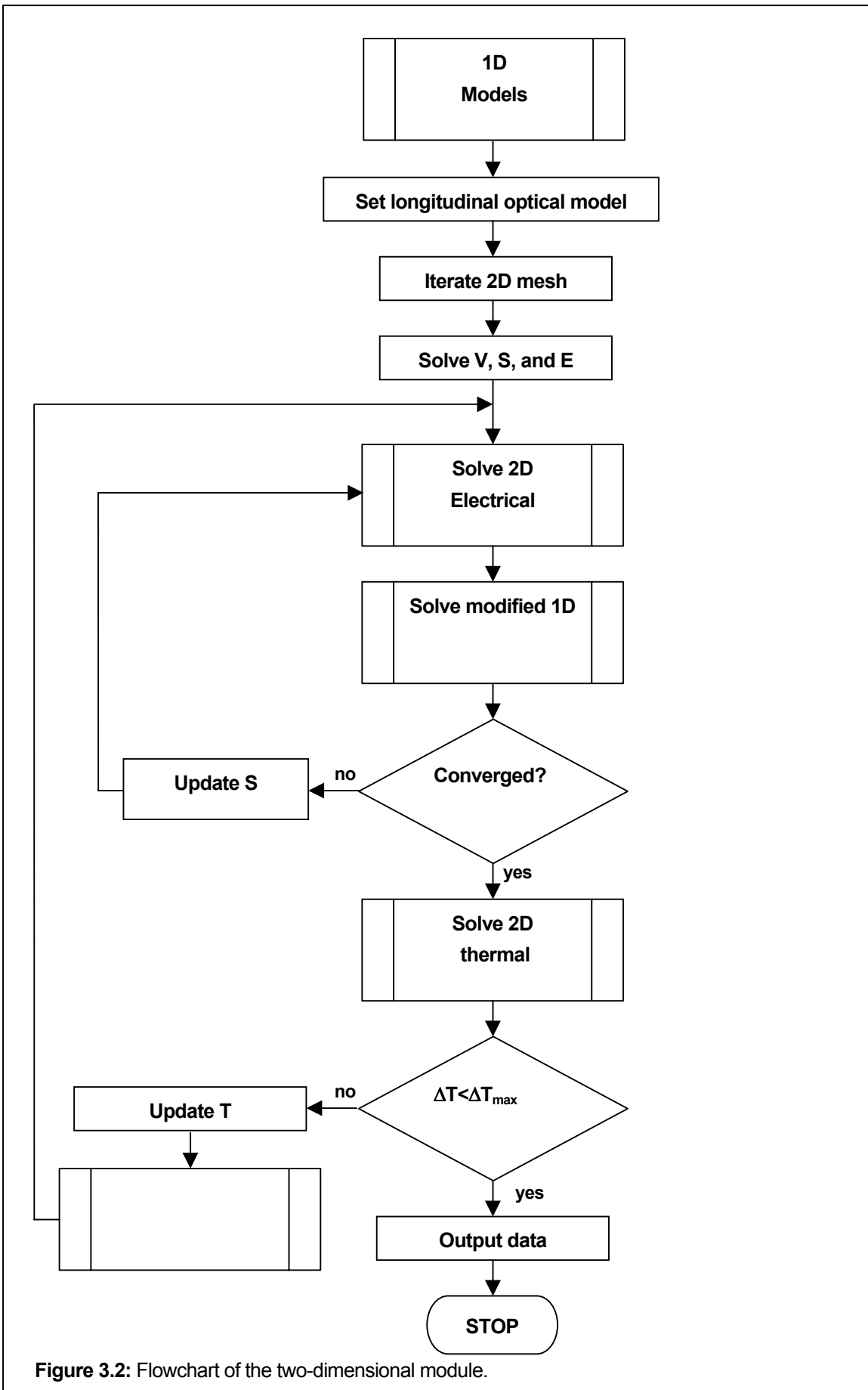
Figure 3.2: Flowchart of the two-dimensional module.

3.3   Basic Equations

The basic equations that describe the behavior of the optoelectronic device are Poisson's equation

$$\nabla \cdot (\varepsilon_d \nabla \phi) + q(p_T - n_T + N_D - N_A) = 0, \tag{3-1}$$

the continuity equations for electrons and holes

$$\nabla \cdot \mathbf{j}_n - q(R^{SRH} + R^{Spont} + R^{Auger} + R_n^{net}) = 0 \tag{3-2}$$

$$\nabla \cdot \mathbf{j}_p + q(R^{SRH} + R^{Spont} + R^{Auger} + R_p^{net}) = 0, \tag{3-3}$$

the capture/escape balance equations (at each quantum well)

$$\frac{1}{q}\nabla \cdot \mathbf{j}_n^{(2D)} - (R_{qw}^{SRH} + R_{qw}^{Spont} + R_{qw}^{Auger} + R^{Stim} + \frac{1}{d_w}\int_{QW} R_n^{net} dy) = 0 \tag{3-4}$$

$$\frac{1}{q}\nabla \cdot \mathbf{j}_p^{(2D)} + (R_{qw}^{SRH} + R_{qw}^{Spont} + R_{qw}^{Auger} + R^{Stim} + \frac{1}{d_w}\int_{QW} R_p^{net} dy) = 0, \tag{3-5}$$

and the photon rate equation

$$(g_m - b_m)S + \frac{\beta}{v_g v}\int R_{qw}^{Spont} dv = 0 \tag{3-6}$$

The above set of nonlinear coupled integral-differential equations is solved self-consistently for the independent variables $\phi, \phi_n, \phi_p, \phi_{nw}, \phi_{pw}$, and ϕ_s, where

$$S = S_0 \left(e^{\phi_s/kT} - 1\right)$$

In addition, we also need to solve the waveguide equation

$$\nabla^2 W + k_0^2 \left(\in - \beta_0^2\right) W = 0 \tag{3-7}$$

to complete the description of the optical characteristics.

Symbol definitions are listed in the Glossary.

3.4   Carrier statistics and current relations

3.4.1   Bulk Region

The carrier density in bulk materials is calculated using Boltzmann statistics. The electron and hole density, respectively, take the form

$$n = n_r \exp\left[\frac{q}{kT}(\phi - \phi_n + \theta_n)\right] \tag{3-8}$$

$$p = n_r \exp\left[-\frac{q}{kT}(\phi - \phi_p + \theta_p)\right] \tag{3-9}$$

with band parameters given by,

$$\theta_n = \frac{(X - X_r)}{q} + \frac{kT}{q} \log\left(\frac{N_c}{n_r}\right) \tag{3-10}$$

$$\theta_p = \frac{(X - X_r)}{q} + \frac{E_g}{q} + \frac{kT}{q} \log\left(\frac{N_v}{n_r}\right). \tag{3-11}$$

The effective density of states for the unconfined (bulk) carriers are given by

$$N_c = 2\left(\frac{2\pi m_n kT}{h^2}\right)^{3/2} \tag{3-12}$$

$$N_v = 2\left(\frac{2\pi m_p kT}{h^2}\right)^{3/2}, \tag{3-13}$$

while the intrinsic carrier density takes the form

$$n_i = \sqrt{N_c N_v} \exp\left(-\frac{E_g}{2kT}\right). \tag{3-14}$$

The intrinsic Fermi energy is given by,

$$E_{F_i} = -\left[q\phi + (X - X_r) + \frac{1}{2}E_g + \frac{1}{2}kT \log\left(\frac{N_c}{N_v}\right)\right] \tag{3-15}$$

The current relations can be expressed in terms of the quasi-Fermi potentials as

$$j_n = -q\mu_n n\left(\nabla \phi_n + P_n \nabla T\right) \tag{3-16}$$

$$j_p = -q\mu_p p\left(\nabla \phi_p + P_p \nabla T\right) \tag{3-17}$$

Note that only unconfined (3D) carriers will contribute to the current.

3.4.2 Quantum Well Region

In quantum well regions, the carrier density of the confined (2D) carriers is calculated using full Fermi-Dirac statistics. Thus, the total electron density is given by

$$n_T = n + n_w \tag{3-18}$$

$$n_w = kT \sum_j (\int_{dw} |\psi_j^e|^2 dy)\rho_j \log\left\{1 + \exp\left[\frac{q}{kT}\left(\phi - \phi_{nw} - \frac{E_j^0}{q} + \theta_{nw}\right)\right]\right\}. \tag{3-19}$$

where ϕ_{nw} is a quasi-Fermi potential *associated with the confined carriers.*

Similarly, the hole density can be expressed as

$$p_T = p + p_w \tag{3-20}$$

$$p_w = kT \sum_i (\int_{dw} |\psi_i^h|^2 dy)\rho_i \log\left\{1 + \exp\left[-\frac{q}{kT}\left(\phi - \phi_{pw} - \frac{E_i^0}{q} + \theta_{pw}\right)\right]\right\}. \tag{3-21}$$

where the quasi-Fermi potential *associated with the confined holes* is denoted by ϕ_{pw}. The summation over i runs over states in both light and heavy hole sub-bands.

The effective density of states for the confined carriers is given by

$$\rho_i = \frac{m_i}{\pi \hbar^2 d_w}$$

where m_i is the carrier effective mass.

The band parameters in quantum well regions are given by

$$\theta_{nw} = \frac{(\chi - \chi_r)}{q} \tag{3-22}$$

$$\theta_{pw} = \frac{(\chi - \chi_r)}{q} + \frac{E_g}{q} \tag{3-23}$$

The energy levels of the quantum well, E_i^0, E_j^0, are defined positive and referred to the band edges. The energy levels are determined *at the beginning* and used throughout the entire simulation.

The user has the option, however, to enter externally the energy levels and the effective masses for each band/sub-band (see section 5.6).

In the quantum well, the form of the intrinsic carrier is similar to that of eq. (3-14), i.e.,

$$n_{iw} = \sqrt{N_{cw} N_{vw}} \, \exp\left(-\frac{E_g}{2kT}\right) \tag{3-24}$$

where the effective density of states for electrons and holes in the quantum well are given by,

$$N_{cw} = kT \sum_j \rho_j \exp\left(-\frac{E_j^0}{kT}\right) \tag{3-25}$$

$$N_{vw} = kT \sum_i \rho_i \exp\left(-\frac{E_i^0}{kT}\right). \tag{3-26}$$

while the intrinsic Fermi energy is

$$E_{F_i w} = -\left[q\phi + (X - X_r) + \frac{1}{2} E_g + \frac{1}{2} kT \log\left(\frac{N_{cw}}{N_{vw}}\right) \right] \tag{3-27}$$

3.5 Recombination

Depending on whether the region is bulk or quantum well HAROLD treats the recombination accordingly.

3.5.1 Bulk regions

The recombination process arises by three mechanisms: Shockley-Read-Hall recombination, spontaneous emission and Auger emission, given by

$$R^{SRH} = \frac{\left(np - n_i^2\right)}{\tau_{p0}\left(n + n_i\right) + \tau_{n0}\left(p + n_i\right)} \tag{3-28}$$

$$R^{Spont} = B\left(np - n_i^2\right) \tag{3-29}$$

$$R^{Auger} = \left(C_n n + C_p p\right)\left(np - n_i^2\right) \tag{3-30}$$

For the case of layers with external definition of deep trap parameters, eq. (3-28) is replaced by the more general expression

$$R^{SRH} = \sum_k \frac{\left(np - n_i^2\right)}{\tau_{pk}\left[n + n_i g_k \exp\left(\frac{E_k - E_{int}}{kT}\right)\right] + \tau_{nk}\left[p + n_i g_k^{-1} \exp\left(\frac{E_{int} - E_k}{kT}\right)\right]} \tag{3-31}$$

The meaning of the quantities appearing in the equations is described in the Glossary. The electron and hole lifetimes are respectively given by,

$$\tau_{nk} = \left[\sigma_{nk}(T)\langle v_n \rangle N_k\right]^{-1} \tag{3-32}$$

$$\tau_{pk} = \left[\sigma_{pk}(T)\langle v_p \rangle N_k\right]^{-1} \tag{3-33}$$

where

$$\sigma_{nk} = \sigma_{nk}^0 \exp\left[E_{ak}\left(\frac{1}{kT_0} - \frac{1}{kT}\right)\right] \tag{3-34}$$

$$\sigma_{pk} = \sigma_{pk}^0 \exp\left[E_{ak}\left(\frac{1}{kT_0} - \frac{1}{kT}\right)\right] \tag{3-35}$$

$$\langle v_n \rangle = \sqrt{\frac{8kT}{\pi m_n}}$$

$$\langle v_p \rangle = \sqrt{\frac{8kT}{\pi m_p}} .$$

3.5.2 Quantum well regions

In quantum wells, eqs (3-28), (3-30) and (3-31) account for Shockley-Read-Hall and Auger processes. The difference is that the carrier densities, the intrinsic carrier density and Fermi energy is replaced by the quantum expressions, eqs. (3-19), (3-21), (3-24) and (3-27). The spontaneous emission, instead, is given by eq. (3-61).

The rate of stimulated recombination is expressed as

$$R^{Stim} = v_g G_{max} S_w$$

where $G_{max} = G(\hbar\omega)$ corresponds to the maximum value of the gain, eq. (3-52). The density of photons in the quantum well, S_w, is given by

$$S_w = \frac{1}{d_w} \int_{QW} S(y)dy$$

where $S(y)$ is the local density of photons, eq. (3-51). Note that the stimulated recombination may eventually become negative at low bias. Nevertheless, its absolute value is always negligible in comparison with the other recombination mechanisms.

3.6 Facet Recombination

The facets of a laser, such as cleaved mirrors or etched mirrors, are subject to an intense nonradiative recombination. The standard assumption is that the origin of such nonradiative recombination lies on the existence of deep trap levels at the surface. For a single dominating surface trap level, the SRH recombination is given by:

$$R^{SURF} = \frac{\left(n_s p_s - n_i^2\right)}{s_{0p}^{-1}\left[n_s + n_{Ts}\right] + s_{0n}^{-1}\left[p_s + p_{Ts}\right]} \tag{3-36}$$

where

$$n_{Ts} = gn_i \exp\left(\frac{E_{Ts} - E_{Fi}}{kT}\right) \tag{3-37}$$

$$p_{Ts} = g^{-1}n_i \exp\left(\frac{E_{Fi} - E_{Ts}}{kT}\right) \tag{3-38}$$

$$s_{0n} = \sigma_{ns}\langle v_n\rangle N_{Ts} \tag{3-39}$$

$$s_{0p} = \sigma_{ps}\langle v_p\rangle N_{Ts} \tag{3-40}$$

Correspondingly, the surface charge density is given by,

$$Q^{SURF} = -qN_{Ts}\frac{s_{0n}\left(n_s - n_{Ts}\right) - s_{0p}\left(p_s - p_{Ts}\right)}{s_{0n}\left(n_s + n_{Ts}\right) + s_{0p}\left(p_s + p_{Ts}\right)} \tag{3-41}$$

The intrinsic surface recombination velocity S_0, defined as a pre-factor to excess minority concentration in the recombination, and the electron and hole surface recombination velocities, S_n and S_p, can be readily obtained from (3-36) as

$$S_0 = \frac{R^{SURF}}{\sqrt{n_s p_s}} \tag{3-42}$$

$$S_n = S_0\sqrt{\frac{p_s}{n_s}} \tag{3-43}$$

$$S_p = S_0\sqrt{\frac{n_s}{p_s}} \tag{3-44}$$

In the present model, eqs. (3-36) and (3-41) are implemented as boundary conditions for the drift-diffusion and Poisson's equations, respectively, at the laser facets. Therefore, at $z = 0$ and $z = L_z$ we impose

$$j_n \cdot n = R^{SURF} \tag{3-45}$$

$$\mathrm{j}_p \cdot n = -R^{SURF} \tag{3-46}$$

$$\nabla \phi \cdot n = \frac{Q^{SURF}}{\varepsilon}, \tag{3-47}$$

where n is the unit vector normal to the surface.

3.7   Capture/Escape Model

One important feature implied by eqs. (3-4) and (3-5) is the fact that, in quantum well regions, the confined (or 2D) carriers are not assumed a *priori* to be in thermal equilibrium with the corresponding unconfined (or 3D) carriers. This becomes essential in order to simulate two basic experimental features occurring above threshold: the increase of the confinement layer spontaneous recombination and the non saturation of the external voltage in structures with high escape times. Obviously, these facts can not be accounted for by a model which assumes thermal equilibrium between 3D and 2D carriers, since the clamping of the 2D carrier density (n_{2d}, p_{2d}) at threshold induces a similar clamping on the 3D carrier density (p_{3d}, n_{3d}).

The capture/escape model considers two distinct quasi-Fermi levels at the QW regions. This feature has been already introduced in Section 3.3. The equilibrium between 3D and 2D carriers is governed by the capture/escape balance equations, eqs. (3-4) and (3-5). The net recombination terms are given by,

$$R_n^{net} = \frac{n_{3d}}{\tau_n^{cap}} - \frac{n_{2d}}{\tau_n^{esc}} \tag{3-48}$$

for electrons, and

$$R_p^{net} = \frac{p_{3d}}{\tau_p^{cap}} - \frac{p_{2d}}{\tau_p^{esc}} \tag{3-49}$$

for holes. These expressions are a consequence of assuming a local capture rate proportional to the density of unconfined carriers, and a local escape rate proportional to the density of confined carriers with total energy greater than the barrier energy.

The 3D carrier properties (band edge, band gap, mobilities, effective masses, etc.) correspond to the material given by the first energy level with energy higher than the barrier energy.

The relationship between the capture time and escape time are assumed as:

$$\frac{\tau_n^{cap}}{\tau_n^{esc}} = \frac{N_c}{kT \sum_i \rho_i \exp[(E_c - E_i)/kT]} \quad \text{and}$$

$$\frac{\tau_p^{cap}}{\tau_p^{esc}} = \frac{N_v}{kT \sum_j \rho_j \exp[(E_j - E_v)/kT]}$$

You can change τ^{cap} in the user interface. The values will influence the laser threshold and slope efficiency above threshold.

3.8   Optical Mode

The distribution of photons within the (two-dimensional) laser cavity is determined by the optical field laser eigenmode.

In the vertical (y) direction, the optical mode profile is found by solving the wave equation, eq. (3-7), using the so-called passive vertical structure approximation. The wave equation is then reduced to

$$\frac{\partial^2 W_R}{\partial y^2} + k_{0e}^2 \left(\overline{n}^2 - n_{eff}^2 \right) W_R = 0 \tag{3-50}$$

where W_R is the real part of the optical field. In a laser structure W_R must vanish far from the active region. Therefore, we impose that $W_R(y=0) = W_R(y=L_y) = 0$, as boundary conditions for eq.(3-50). The solution of the associated eigenvalue problem yields the various modes of the cavity. The transverse distribution of photons in a given eigenmode is given by

$$f_T(y) = |W_R|^2$$

In order to single out the lasing mode we further impose the following restrictions[1]:

a) The maximum value of $|W_R|^2$ must lie within the confinement region (see Section 3.10.3) or quantum well region (see Section 3.10.2).

b) From all solutions fulfilling condition (a), the one having the largest effective index is chosen.

c) The transverse mode is normalized to unity, *i.e.*,

$$\frac{1}{L_y} \int_0^{L_y} f_T(y) dy = 1$$

On the other hand, the strength of the optical field along the cavity axis (z) is proportional to,

---

[1] The user is advised to check the optical mode profile in order to ensure that the solution yielded by the program is satisfactory. This can be plotted by running the program in "Test" mode (see Execution Mode).

$$f_L(z) = \frac{\alpha_m L_z}{2\sinh\left(\frac{\alpha_m L_z}{2}\right)\left(1 + \sqrt{\frac{R_1}{R_2}}\right)}\left[\exp(-\alpha_m z) + \sqrt{\frac{R_1}{R_2}}\exp(\alpha_m z)\right]$$

where we have neglected the influence of the mirror absorption.

The product $f_T(y)f_{L(z)}$ gives the probability of finding a photon at position (x, y). Therefore, the *local* density of photons can be written

$$S(x, y) = f_T(y)f_L(z)\langle S \rangle. \tag{3-51}$$

3.9   Boundaries and contacts

HAROLD handles two types of boundary conditions for the electrical equations, eqs. (3-1), (3-2), and (3-3) : purely voltage controlled ohmic contacts and current controlled contacts.

3.9.1 Ohmic contacts

The boundary condition for ohmic contacts is implemented as a Dirichlet boundary condition.

Left Contact	Right Contact	Equation
$\phi - \phi_b = 0$	$\phi - \phi_b - V_d = 0$	Poisson
$\phi_n - \phi + \phi_b = 0$	$\phi_n - \phi + \phi_b = 0$	Electron Continuity
$\phi_p - \phi + \phi_b = 0$	$\phi_p - \phi + \phi_b = 0$	Hole Continuity

Here ϕ_b is the built-in potential. Note that the term "device voltage" excludes the substrate, *i.e.*, it represents the voltage difference *due to the layers only*. Moreover, it is taken relative to the junction between the substrate and the first layer of the device.

3.9.2 Current controlled contacts

When a semiconductor laser device is biased beyond threshold, the optical gain and carrier concentrations practically saturate, causing the saturation of the bias voltage. The current, though, continues to rise due to the stimulated emission. Therefore, it becomes essential in the simulation to implement the possibility to control the biasing of the device through current injection instead of voltage. This can be achieved by replacing the above boundary condition of the Poisson's equation by

$$j_n + j_p - J_{ext} = 0$$

at the right contact. Here, the ϕ dependence enters implicitly in the definition of the currents, eqs. (3-16) and (3-17).

3.10 Layer Type

HAROLD distinguishes the following types of layers: *bulk, confinement, quantum well, substrate,* and *metal* layers. These are specified by the user in the epitaxial layer structure editor, as described in Section 4.2. This section will explain the way they are treated by the program.

3.10.1 Bulk

The main characteristic of a *bulk layer* is that carrier densities follow Boltzmann statistics, as expressed by eqs. (3-8) and (3-9). No distinction between light hole and heavy hole sub-bands are made. Thus, only two bands are treated: conduction and valence. The hole effective mass m_p is given by

$$m_p^{3/2} = m_{lh}^{3/2} + m_{hh}^{3/2}.$$

Only spontaneous, Shockley-Read-Hall, and Auger processes are considered. Furthermore, a bulk region does not contribute to the gain. Bandgap narrowing is due to impurity ionization only.

Typically, cladding layers are treated as bulk.

3.10.2 Quantum Well

In contrast to a *bulk layer*, the carrier density in a *quantum well layer* consists of two contributions:

1. Confined (n_w, p_w) carriers following Fermi-Dirac statistics, eqs. (3-19) and (3-21)

2. Unconfined (n, p) carriers following Boltzmann statistics (as in bulk layers)

The properties of the unconfined carriers in a *quantum well layer* (i.e. band edges, band gap, mobilities, effective masses, etc.) correspond to those of the associated confinement layer at the barrier.

The equilibrium between unconfined and confined carriers is described by the capture/escape balance equations (Section 3.7). Confined (2D) carriers contribute to the optical gain.

Obviously, an active layer must be labeled as *quantum well*.

3.10.3 Confinement

A *confinement layer* is a layer adjacent to a *quantum well layer*. It serves two purposes:

1. to define the relevant optical waveguide of the lasing cavity, and

2. to provide a spatial scale at which the wavefunctions corresponding to the bound states of the quantum well vanish.

In all remaining aspects they are treated as *bulk* regions. It should be noted that a *quantum well* layer must *always* be surrounded by *confinement* layers.

Typically, a GRIN structure would be defined as a *confinement* layer. In the case of multiple quantum well structures, the regions between quantum wells must be defined as *confinement* layer.

3.11 Bandgap Narrowing

Emission at wavelengths longer than predicted from the knowledge of the energy levels has been observed in quantum well lasers. A possible explanation of this effect is a reduction of the bandgap at high carrier densities due to many-body interactions. This reduction is taken to vary proportionally to the 1/3 power of the carrier density.

In quantum well regions the reduction in of the bandgap is given by

$$\Delta E_g = -\Delta E_0^{(qw)} \left(\frac{n+p}{2} \right)^{\frac{1}{3}}$$

In bulk regions, the reduction bandgap narrowing depends on the density of ionized impurities, and can be expressed by,

$$\Delta E_g = \begin{cases} -\Delta E_0^{(n)} N_D^{1/3} & n-type \\ -\Delta E_0^{(p)} N_A^{1/3} & p-type \end{cases}.$$

3.12 Strain

Strained regions are incorporated into the current version of the program via the approach of Krijn for the band offsets. Here, the conduction and valence band energies are obtained on an absolute scale from

$$E_v = E_{v,av} + \frac{E_{so}}{3} + \Delta E_{v,av}^{hy} + \max\left(\Delta E_{hh}^{sh}, \Delta E_{lh}^{sh} \right)$$

$$E_c = E_{v,av} + \frac{E_{so}}{3} + E_g + \Delta E_c^{hy}$$

where

$$\Delta E_{hh}^{sh} = -\frac{1}{2} \delta E^{sh}$$

$$\Delta E_{lh}^{sh} = -\frac{1}{2} E_{so} + \frac{1}{4} \delta E^{sh} + \frac{1}{2} \left[E_{so}^2 + E_{so} \delta E^{sh} + \frac{9}{4} \left(\delta E^{sh} \right)^2 \right]^{\frac{1}{2}}.$$

The quantities $E_{v,av}, E_{so}$, and E_g refer to unstrained bulk properties. The strain contribution is incorporated in $\Delta E_{v,av}^{hy}, \Delta E_c^{hy}, \Delta E_{lh}^{sh}$ and ΔE_{hh}^{sh}. The first two quantities and δE^{sh} can be conveniently parameterized as a function of the alloy concentrations of the quaternary material and included in the material database. Together with the affinity and the bandgap, the band structure of the strained material can be obtained.

It should be mentioned that those equations were obtained by treating the effect of strain as a small perturbation, and are therefore valid in the case of small lattice mismatch.

3.13 Gain and Spontaneous Recombination Model

3.13.1 Gain

The interband local gain, due to all possible transitions from conduction band states j, to valence band states i, is given by,

$$g(E) = \gamma_g \frac{\pi q^2 \hbar}{nc\,\varepsilon_0\, m_e} M_0^2 \frac{1}{E} \sum_{j=i} C_{ij} A_{ij}^{pol}(E) \rho_{ij} \left[f_j(E) - f_i(E) \right] \tag{3-52}$$

where E is the energy of the emitted photon, C_{ij} is the overlap integral of the transition state i and j,

$$C_{ij} = \int_{dw} |\psi_i(y)\| \psi_j(y)| \, dy$$

and $\overline{n}$ is the real part of the refractive index. The summation runs over allowed transitions, which implies that the states involved must have the same quantum numbers. Both light hole and heavy hole sub-band states are included in the summation. M_0^2 is the dipole moment of the bulk material given by,

$$M_0^2 = \frac{1}{6}\left(\frac{1}{m_n'} - 1 \right) \frac{E_g(E_g + E_{so})}{E_g + \frac{2}{3}E_{so}} \tag{3-53}$$

In the above expression, m_n' is a *corrected* effective electron mass which accounts also for gain effects due to higher and lower bands.

The Fermi occupation factors, $f_j(E)$ and $f_i(E)$, can be expressed in terms of the quasi-Fermi potentials associated to the confined carriers as,

$$f_j(E) = \left\{ 1 + \exp\left[-\frac{q}{kT}\left(\theta_{nw} - \frac{E_j^0}{q} - \frac{m_{ij}}{m_j}\frac{(E - E_{ij})}{q} - \phi_{nw} \right) \right] \right\}^{-1} \tag{3-54}$$

$$f_i(E) = \left\{ 1 + \exp\left[-\frac{q}{kT}\left(\theta_{pw} - \frac{E_i^0}{q} - \frac{m_{ij}}{m_i}\frac{(E - E_{ij})}{q} - \phi_{pw} \right) \right] \right\}^{-1}. \tag{3-55}$$

The dipole moment enhancement factors are given by,

$$A_{ji}^{pol}(E) = a_{ij}^{pol} + b_{ij}^{pol}\left(\frac{E_{ij}}{E} \right) \tag{3-56}$$

for $E \geq E_{ij}$. The values of the coefficients a_{ij}^{pol} and b_{ij}^{pol} for the cavity modes and valence sub-bands are listed in Table 3.1. TE is the built in default. The user may switch to TM by turning on the appropriate option in the device editor (see Section 5.2).

Mode	Band	a_{ij}^{pol}	b_{ij}^{pol}

TE	HH	3/4	3/4
TE	LH	5/4	-3/4
TM	HH	3/2	-3/2
TM	LH	1/2	3/2

Table 3.1: Polarization coefficients

The gain broadening caused by intra-band scattering is described by means of the convolution of the optical gain, eq.(3-52), with a line shape function,

$$G(\hbar\omega) = \int g(E)L(\hbar\omega - E)dE..$$

(3-57)

A Lorentzian function is used for the line shape

$$L(x) = \frac{1}{\pi}\frac{\gamma}{\gamma^2 + x^2}$$

(3-58)

with a constant width given by

$$\gamma = \frac{\hbar}{\tau_{in}}.$$

(3-59)

τ_{in} is called intraband relaxation time (**intrabandRelaxTime**). Typically τ_{in} takes values in the range of 0.1~0.2 ps.

The modal gain, appearing in eq.(3-6), is calculated from eq.(3-57) through the expression

$$g_m = \int G(\hbar\omega)f_{opt}(y)dy.$$

The total losses are given by,

$$b_m = \alpha_m + \alpha_{scat} + \alpha_{fc}$$

(3-60)

where

$$\alpha_{fc} = \int \left(\alpha_{fn}^0 n_T + \alpha_{fp}^0 p_T\right)f_{opt}(y)dy$$

accounts for the losses arising from the absorption of photons due to free carriers.

3.13.2 Spontaneous recombination

Near threshold the current is mainly determined by the spontaneous emission rate. The expression given by eq. (3-29) is only valid outside quantum well regions. In the presence of a quantum well, the total spontaneous recombination rate is given by the expression,

$$R_{qw}^{Spont} = \int r_{sp}(E)dE$$

(3-61)

where

$$r_{sp}(E) = \gamma_{sp}\frac{q^2\overline{n}^3 E}{\pi\hbar^2 m_e^2 c^3 \varepsilon}M_0^2\sum_{ji}C_{ij}\rho_{ij}f_j(E)(1 - f_i(E)),$$

(3-62)

consistent with the gain model described in the previous section. Here, the sum runs over all band and sub-band quantum states. The factor γ_{sp} (**sponRecombFac**) has been

added as an *ad-hoc* parameter. It enables the user to exercise an overall control of the amount of spontaneous recombination without altering the remaining quantities (see Section 5.2).

The spectrum of spontaneous emission is calculated according to

$$R_{qw}^{Spont}(\hbar\omega) = \int r_{sp}(E)L(\hbar\omega - E)dE \tag{3-63}$$

where $L(x)$ is the Lorentzian shape function, defined by eq. (3-58).

3.14 Optical characteristics

At each bias level HAROLD obtains, from the solution of the photon rate equation, the total number of photons S that are present in the laser cavity. Thus, the *total* optical power generated in the device is given by

$$P_{opt} = v_g \alpha_m \hbar\omega_0 S \tag{3-64}$$

where the photon energy $\hbar\omega_0$ corresponds to the maximum of the gain spectrum, eq. (3-57).

The output power through each facet is actually a fraction of the total optical power, since it is limited by both the absorption and the scattering losses at the mirror facets. The output power per facet is calculated as,

$$P_{opt}^{(1)} = \frac{\left(1 - \alpha_m^{(1)}\right)\left(1 - s_m^{(1)} - r_m^{(1)}\right)}{\left(1 - r_m^{(1)}\right) + \sqrt{\dfrac{r_m^{(1)}}{r_m^{(2)}}\left(1 - r_m^{(2)}\right)}} P_{opt} \tag{3-65}$$

$$P_{opt}^{(2)} = \frac{\left(1 - \alpha_m^{(2)}\right)\left(1 - s_m^{(1)} - r_m^{(1)}\right)}{\left(1 - r_m^{(2)}\right) + \sqrt{\dfrac{r_m^{(2)}}{r_m^{(1)}}\left(1 - r_m^{(1)}\right)}} P_{opt} \tag{3-66}$$

3.15 Thermal Model

3.15.1 Heat Flow Equation

The variation of the temperature distribution as the device is biased is described by the heat flow equation (HFEQ),

$$\nabla \cdot J_Q = w. \tag{3-67}$$

Here, J_Q represents the heat current, and is given by the expression,

$$J_Q = -\kappa\nabla T, \tag{3-68}$$

where κ is the thermal conductivity.

The vertical boundary conditions are given by,

$$J_Q \cdot e_y \big|_{boundary} = \left|\frac{T_{boundary} - T_{HS}}{\rho_{th}}\right|$$

which represents the magnitude of the heat flow that goes into the heat sink, while the parameters T_{HS}, the heat sink temperature, and ρ_{th}, the effective thermal resistivity,

allow to simulate the heat sink properties in a simple way. The effective thermal resistivity is constructed as,

$$\rho_{th} = \rho_{thc} + L_x L_z R_{ths} \tag{3-69}$$

The boundary conditions at the mirror facets are given by,

$$J_Q \cdot e_z \big|_{mirror} = w_{SURF} + w_{ABS}$$

where

$$w_{SURF} = qR_{SURF}\left[(\phi_n - \phi_p) + T(P_n + P_p)\right] \tag{3-70}$$

is the heat per unit area due to surface recombination, while

$$w_{ABS} = P_{ABS}\frac{f_T(y)}{L_x L_y}$$

is the heat generated per unit area due to photon absorption at the facet.

The local density of heat sources, w, arise from the various power dissipation mechanisms which are present in the device,

$$w = w_{joule} + w_{nr} + w_{fc} + w_{exc}. \tag{3-71}$$

The following local heating mechanisms are considered:

Joule heating

In *bulk*, *confinement* and *quantum well* regions, it is calculated as,

$$w_{joule} = \frac{1}{q}\left(\frac{j_n^2}{\mu_n n} + \frac{j_p^2}{\mu_p p}\right)^2. \tag{3-72}$$

For *metal* and *substrate* regions, it is given by,

$$w_{joule} = \rho_{el}\left(j_n + j_p\right)^2.$$

The heat released at the contacts is calculated as,

$$w_c^{(1)} = \frac{\rho_c^{(1)}}{\delta y}\left(j_n + j_p\right)^2$$

for the first metal/non-metal interface encountered in the device file, and

$$w_c^{(2)} = \frac{\rho_c^{(2)}}{\delta y}\left(j_n + j_p\right)^2$$

for the first non-metal/metal interface encountered.

Non-radiative recombination For *bulk*, *confinement* and *quantum well* regions, it is given by,

$$w_{nr} = q\left(R^{SRH} + R^{Auger}\right)\left[(\phi_n - \phi_p) + T(P_n + P_p)\right] \tag{3-73}$$

Photon absorption by to free carriers For *bulk*, *confinement* and *quantum well* regions, it is given by,

$$w_{fc} = \left(\alpha_{fn}^0 n_T + \alpha_{fp}^0 p_T\right)Sf_{opt}v_g L_y \hbar\omega. \tag{3-74}$$

Power excess The power excess, w_{exc}, has been introduced in order to account for all remaining power dissipation mechanisms. The total power dissipated

by the whole device including the substrate and the metal layers must exactly balance the amount of the external power, IV. Therefore, the average excess power is given by

$$P_{exc} = \int w_{exc} dv = IV - P_{opt.} + P_{scat} - P_{SURF} - \int \left(w_{joule} + w_{nr} + w_{fc} \right) dv, \qquad (3\text{-}75)$$

where the integration extends over the entire device volume. Note that the scattered optical power at the mirror facets is included within the excess power. The conversion of the power excess into heat depends on the absorptive characteristics of the device, and will be discussed in Section 3.15.2.

3.15.2 Absorption

Equation (3-75) defines the total averaged excess power in the entire device (layers+substrate). Currently, HAROLD assumes that the energy of the transitions associated to spontaneous emission (the main source of excess power) is lower than the substrate and p-contact respective band gaps *only*. Therefore, half of averaged excess power will be absorbed at the substrate while the other half will be absorbed at the p-contact layer.

In the substrate the spatial distribution of the (half) averaged power excess is assumed exponential, with an absorption length $1/\alpha_s$, while at the p-contact is considered uniform. Thus,

$$w_{exc}(y) = \begin{cases} \dfrac{1}{2}\left(\dfrac{P_{exc}}{L_x L_z} \right) \alpha_s e^{-\alpha_s |y - y_s|} & \quad substrate \\[2em] \dfrac{1}{2}\left(\dfrac{P_{exc}}{L_x L_z d_p} \right) & \quad p-contact \\[2em] 0 & \quad otherwise \end{cases} \qquad (3\text{-}76)$$

where d_p is the thickness of the p-contact (assumed to be the last *bulk* layer).

Chapter 4

Performing a Simulation

The general procedure to perform a simulation is as follows:

- ➢ Creating a Harold project
- ➢ Setting up the epitaxial layer structure
- ➢ Setting up the device properties
- ➢ Defining trap set (if needed)
- ➢ Defining quantum well levels (if needed)
- ➢ Defining meshing policies (if needed)
- ➢ Setting up and running the simulator

The following sections will explain how to complete these tasks.

4.1   Creating a Harold project

A Harold project contains all the information for a simulation task. You can generate a Harold project by

- ➢ clicking File /New Project menu or
- ➢ right clicking the topmost node in the project window, then in the popup window, selecting Add/Harold Project.

4.2   Setting up the epitaxial layer structure
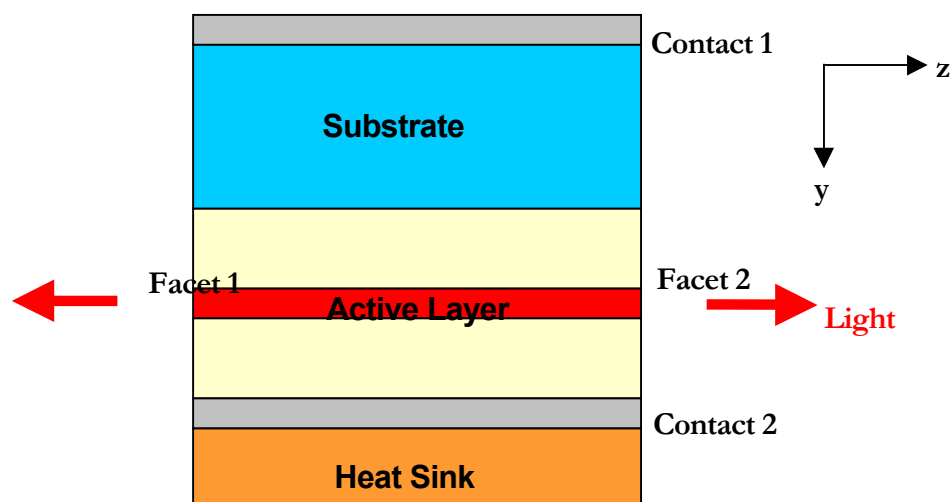
Figure 4.1 Typical geometry of a laser device

The typical geometry of a device is shown in **Figure 4.1**. You can add an epitaxial layer structure to a Harold project and edit it by

➢ right clicking the project node into which you want to put the layers

➢ selecting **Add/Epitaxial Layer Structure** , this will generate an epitaxial layer structure

➢ double clicking the epitaxial layer structure just created, this will bring up the *Epitaxial Layer Structure Editor* (see chapter 5.1 for details) for you to edit the structure

4.3   Setting up the device properties

The other parameters control the way in which Harold behaves is the device properties. You should add a device object and edit it to modify these properties. It can be done by

➢ right clicking the project node into which you want to add the device object

➢ selecting **Add/Device**, this will create a device object

➢ double clicking the device just created, a *Device Editor* will display and you can edit the device (see chapter 5.2 for details)

4.4   Defining trap set

If you like to provide enhanced control of the Shockley-Read-Hall recombination behaviors rather than using the default behaviors, you should define a deep trap set. It can be done by

➢ right clicking the project node into which you want to add an deep trap set

➢ selecting **Add/Trap Definition Set** , this will generate an deep trap set

➢ double clicking the trap set just created, a *Trap Definition Set Editor* will popup for editing the trap set (see chapter 5.5 for details)

4.5   Defining quantum well levels

Harold allows the user to optionally specify quantum well parameters rather than solving the quantum well system. It can be done by

➢ right clicking the project node

➢ selecting **Add/Quantum Well Definition**, this will generate an empty quantum well definition set

➢ double clicking the definition set just created, a *Quantum Well Set Editor* will popup for editing (see chapter 5.6 for details)

4.6   Defining mesh policies

Harold has default mesh policy to generate the mesh for the simulation. But you can add new meshing policy and use it for your simulation. Adding a new meshing policy can be done by

➢ Right clicking the project node

➢ Selecting **Add/Mesh Policy,** this will generate an empty mesh policy

➢ Double clicking the mesh policy just created, a *Mesh Policy Editor* will popup for editing (see chapter 5.7 for details)

4.7   Setting up and running the simulator

The last step for a simulation is to create a Simulator object and running it.

➢ right clicking the project node into which you want to add a simulator

➢ selecting **Add/Simulator**, this will create a simulator object

➢ double clicking the simulator just created, a *Simulator* panel will display, and you can edit the parameters and running the simulator (see chapter 5.3 for details)

Graphical User Interface Reference

5.1   The epitaxial layer structure editor

Figure 5.1 shows the *Epitaxial Layer Structure Editor*. The editor consists of a number of components:
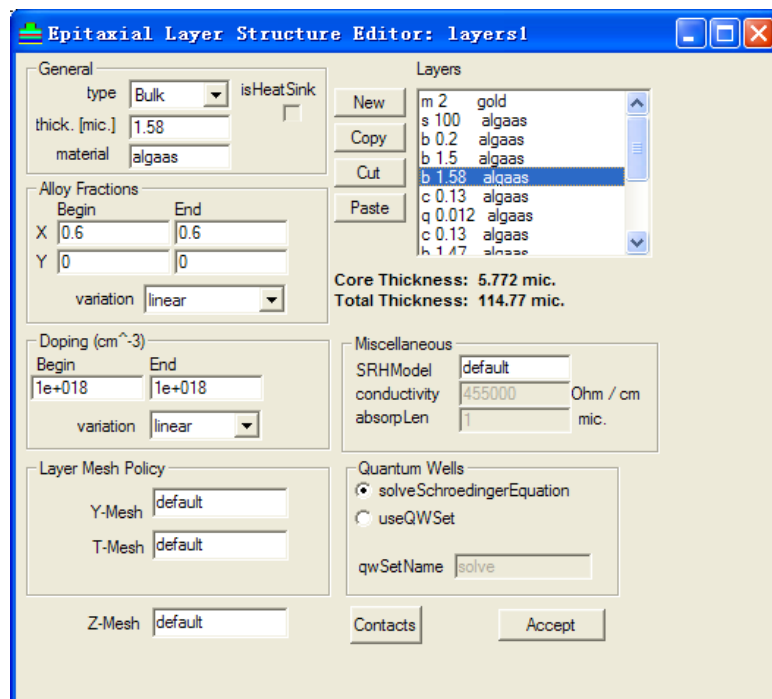
Figure 5.1: The Epitaxial Structure Editor.

- The **Layers** list box**:** This contains a list of the layers starting with the bottom metallic contact, then the substrate and then subsequent layers. Each line of the list contains (from left to right) a character representing the type of layer, the thickness of the layer and the material of the layer. For example, a two-micron layer of gold would be written: "m 2 gold". By selecting a line in the list, the editor enables or disables those properties that are not relevant to the type of layer that has been selected. You can add or remove layers by using the New , Copy , Cut and Paste buttons on the left-hand side of the list. The *core thickness* and the *total thickness* are also shown here. The *core thickness* is defined as the sum of the thicknesses of all *bulk*,

quantum well and *confinement* layers. The *total thickness* is the sum of the thicknesses of all the layers (regardless of what type of layers they are).

- The **General** information box**:** This contains general information about the layer including the layer thickness, the material and the type:

  type chooses the type of the layer selected; See §3.10.

  thick specifies the thickness of the layer in micrometer;

  isHeatSink check this if the layer is a heat sink;

  material specifies the material file name for the layer

- The **Alloy Fractions** box**:** This allows you to specify the start and end point alloy concentration parameters and also how the concentration varies within this region.

  X|Begin specifies the start point alloy concentration for component X;

  X|End specifies the end point alloy concentration for component X;

  Y|Begin specifies the start point alloy concentration for component Y ;

  Y|End specifies the end point alloy concentration for component Y;

  variation specifies how the concentration varies within the layer .

- The **Doping** box**:** This allows you to specify the doping parameters:

  Doping|Begin specifies the start point doping concentration of the layer;

  Doping|End: specifies the end point doping concentration of the layer;

  Doping|variation specifies how the doping concentration varies within the layer.

- The **Quantum Wells** settings box**:** This allows you to choose whether you want HAROLD to solve the Schrödinger Equation for the energy levels in a quantum well structure.

  solveSchrödingerEquation selects it to allow Harold to solve the Schrödinger Equation for the energy levels in a quantum well structure.

  useQWSet: selects it to use a *Quantum well definition set* for the quantum well system.;

  qwSetName: specifies the *Quantum well definition set* name for the quantum well system

- The **Layer Mesh Policy** settings box:

  Y-Mesh: specifies the mesh policy of each layer along y axis for electronic and optical calculation;

  T-Mesh: specifies the mesh policy of each layer along y axis for thermal calculation.

Figure 5.2: The Mesh Policy Editor.

- The **Z-Mesh** setting box: specifies the mesh policy along z axis.

Harold provides default *Mesh Policy* for each kind of layer. Harold will discretise each layer into a number of slices with certain thickness. The number of slices and the

corresponding thickness of a layer is called a *Mesh Policy* as a whole. You can change the default *Mesh Policy* for each layer by assigning it a different one if you like. You can use the *Mesh Policy Editor* (see chapter 5.7 for details.) to make a new *Mesh Policy*.

Setting up the mesh is a delicate step, since the quality of the solution (and the CPU time) relies upon a smart definition of the mesh points.

There are three different meshes in Harold: the electrical mesh (**Y-Mesh**), the thermal mesh (**T-Mesh**), and the longitudinal mesh (**Z-Mesh**).

The region under discretisation can be divided into several mesh-layers (do not need to coincide with the epitaxial layers) in order to allow different mesh point densities, depending on the device structure. The width of the mesh-layer (in microns) and the number of nodes follow, on a layer per layer basis. For a given mesh-layer the node spacing is taken as uniform and is determined by the ratio of the width_of_layer/number_of_nodes, while the first node in the mesh-layer coincides with last node of the previous one.

Electrical mesh (Y-Mesh): This mesh will be used to discretise the semiconductor equations in the vertical (y) direction. The *first* mesh point coincides with the *start of the first bulk*, and the *last* mesh point *must* coincide with the *end of the last bulk layer*. Therefore, *substrate* (s) and *metal* (m) layer types are excluded, while *confinement* (c), *quantum well* (q) and the remaining *bulk* layers are included within the y-mesh.

As a starting point we would recommend the following electrical meshing.

1) From the substrate border to 91% of the n-cladding: 100 points
2) From 91% of the n-cladding to 93% of the n-barrier: 50 points
3) From 93% of the n-barrier to 7% of the p-barrier: 100 points
4) From 7% of the p-barrier to 9% of the p-cladding: 50 points
5) From 9% of the p-cladding to the p contact border: 50 points

Thermal mesh (T-Mesh): This mesh will be used to discretise the heat flow equation in the vertical (y) direction. The *first* mesh point coincides with the *start of the first layer*, and the *last* mesh point *must* coincide with the *end of the last layer*. Therefore, it ranges over all layers of the device (including metals and substrate).

The reason for choosing a different mesh for the discretisation of the heat flow equation relies purely upon optimization arguments. Usually, the number of mesh-points needed to achieve an acceptable solution for the temperature field is much lower than those needed for the electrical potentials, since temperature varies smoothly across heterojunctions.

As a starting point, we would recommend the following thermal meshing:

1) From 0 to n-metal width: 4 points
2) From (1) to (1) + 0.1 μm: 3 points
3) From (2) to (n-metal + substrate - 5 microns): 10 points
4) From (3) to (2)+5 μm: 5 points
5) From (4) to (3)+ n_contact + n_cladding - 0.01 μm: 30 points
6) From (5) to (4)+ 0.01 μm: 10 points
7) From (6) to (5)+ Barriers + QW + p_cladding + p_contact: 22 points
8) From (7) to (6)+0.01 μm: 3 points
9) From (8) to (7) + p_metal - 0.01 μm: 3 points
10) From (9) to (8) + heat_sink: 5 points

Longitudinal mesh (Z-Mesh): The program uses a rectangular mesh to solve the two dimensional problem. This mesh will be used in conjunction with the electrical mesh and the thermal mesh, to discretise the semiconductor equations and the heat flow equation, respectively, in the longitudinal (z) direction. It is therefore relevant only when the simulation is performed in 2-D mode.

The *first* mesh point coincides with the left facet (or facet1) while the *last* mesh point *must* coincide with the right facet (or facet 2).

- The **Contacts** button:

By pressing this button, an editor appears that allows you to specify the resistivities of the contacts.

They are used when an interface between *metal* (m) and semiconductor layer (s or b) is encountered. The order is in correspondence with the layer order.

- The **Miscellaneous** settings box**:**

SRHModel: If 'default' is specified, then eq.(3-28) is used, with the electron and hole lifetimes specified in the device properties (see chapter 5.2) . If the name of a trap definition set is specified, then SRH recombination will use the model of eq.(3-31).

conductivity specifies the electric conductivity of a metal layer or a substrate layer.

absorpLen specifies the power absorption length of a substrate layer in micrometers.

5.2 The device editor
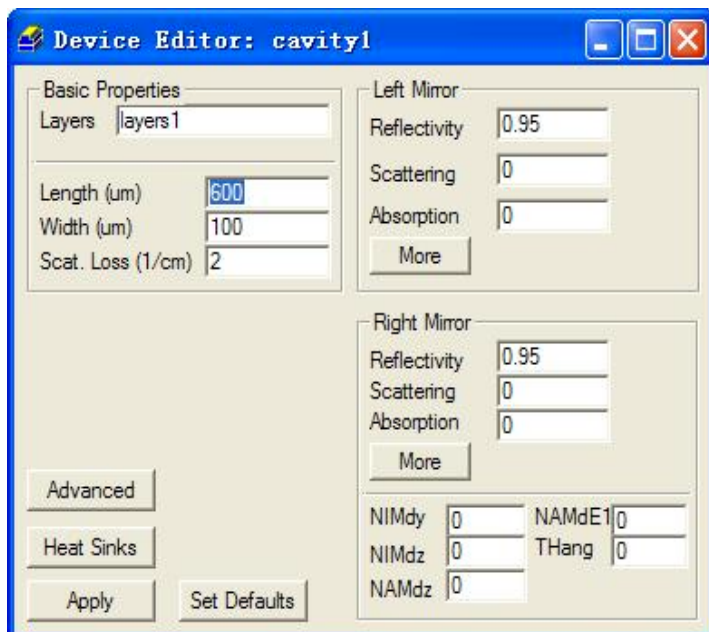
Figure 5.3: The Device Editor

Figure 5.3 shows the Device Editor:

- **Left/Right Mirror Properties:** These boxes allow you to change the properties of the mirrors at either end of the device. Press the More buttons to alter the more advanced properties of the mirrors (properties such as the electron trap cross-section).

- **Basic Properties:** This allows you to set the basic properties of the device such as the width and the length. Here you also specify which epitaxial structure your device is using. To do this, change the "Layers" property to the name of the epitaxial structure node that you desire.

- **Advanced Settings:** Press the Advanced button to get a list of advanced properties which you can then edit. These properties include:

intrabandRelaxTime The value of intraband relaxation time τ_{in} in seconds, eq. (3-59).

squareMatElt	Square of the dipole moment of the bulk material, in eV^2. If set to 0 (default) it will be calculated internally from eq. (3-53) using the electron mass found in the material database.
gainFactor	The factor γ_g in the gain, eq. (3-52).
sponRecomFac	The factor γ_{sp} in the spontaneous recombination, eq. (3-62).
polarization	The polarization of the optical waveguide modes. It also influences the selection of the dipole moment enhancement factors used in the calculation of the gain: TE = Transverse Electric; TM = Transverse Magnetic. See chapter 3.13.1. Default value = TE.
e-SRHLife	Electron lifetime in Shockley-Read-Hall recombination, τ_{n0} in eq. (3-28), in seconds.
h-SRHLife	hole lifetime in Shockley-Read-Hall recombination, τ_{p0} in eq. (3-28), in seconds.
e-CaptureTime	Capture time constant for electrons, τ_n^{cap} in eq. (3-48), in seconds.
h-CaptureTime	Capture time constant for holes, τ_p^{cap} in eq. (3-49), in seconds.
spontEmissCouple	Fraction of the spontaneous emission that couples to the optical mode, β in eq. (3.6).
isLongitudinal	(Only 2D) If false, the optical field in the longitudinal direction (Z) is assumed uniform. If true, the field is calculated as in chapter 3.8. Default value is true
waveOverlap	If TRUE, Harold will consider the overlap integration of electron wavefunction and hole wavefunction in the gain calculation. If false, the overlap integration is ignored.
V-Increment	Increment of the voltage, in *Volts*, from one bias to the next under voltage bias control. Default value = 0.5
switchV	voltage, in *Volts*, at which to switch from voltage-controlled to current-controlled bias (see Section 3.9). If the absolute value of the current at this voltage is larger than the maximum specified current, the program stops. If set to zero (recommended), Harold will set the switch voltage automatically, beginning with a default value = Energy of the first transition E_{11} and, if need be, incrementing this value in steps of 1% until the current has the correct sign when current-controlled biasing begins. Otherwise, the switch voltage will be fixed at the value set by the user [N.B. errors can occur if this is $<\sim E_{11}$; automatic setting is recommended].
e-ThermoPwr	Thermoelectric powers for electrons , in unit of $k/2e$.
h-ThermoPwr	Thermoelectric powers for holes , in unit of $k/2e$.

- **Special facet parameters (only 2D)**

NIMdy	Non-injecting mirror vertical offsets in microns. See **Figure 5.5**
NIMdz	Non-injecting mirror longitudinal offsets in micros. See **Figure 5.5**
NAMdE1	Non-absorbing mirror's increment of the energy corresponding to the fist transition in eV. See **Figure 5.6**
NAMdz	Non-absorbing mirror longitudinal offset in microns. See **Figure 5.6**

THang Offset for thermal overhang in microns. See

Figure 5.4

Figure 5.4 Thermal overhang

Figure 5.5 Non-injecting mirror setup

Figure 5.6 Non-absorbing mirror setup
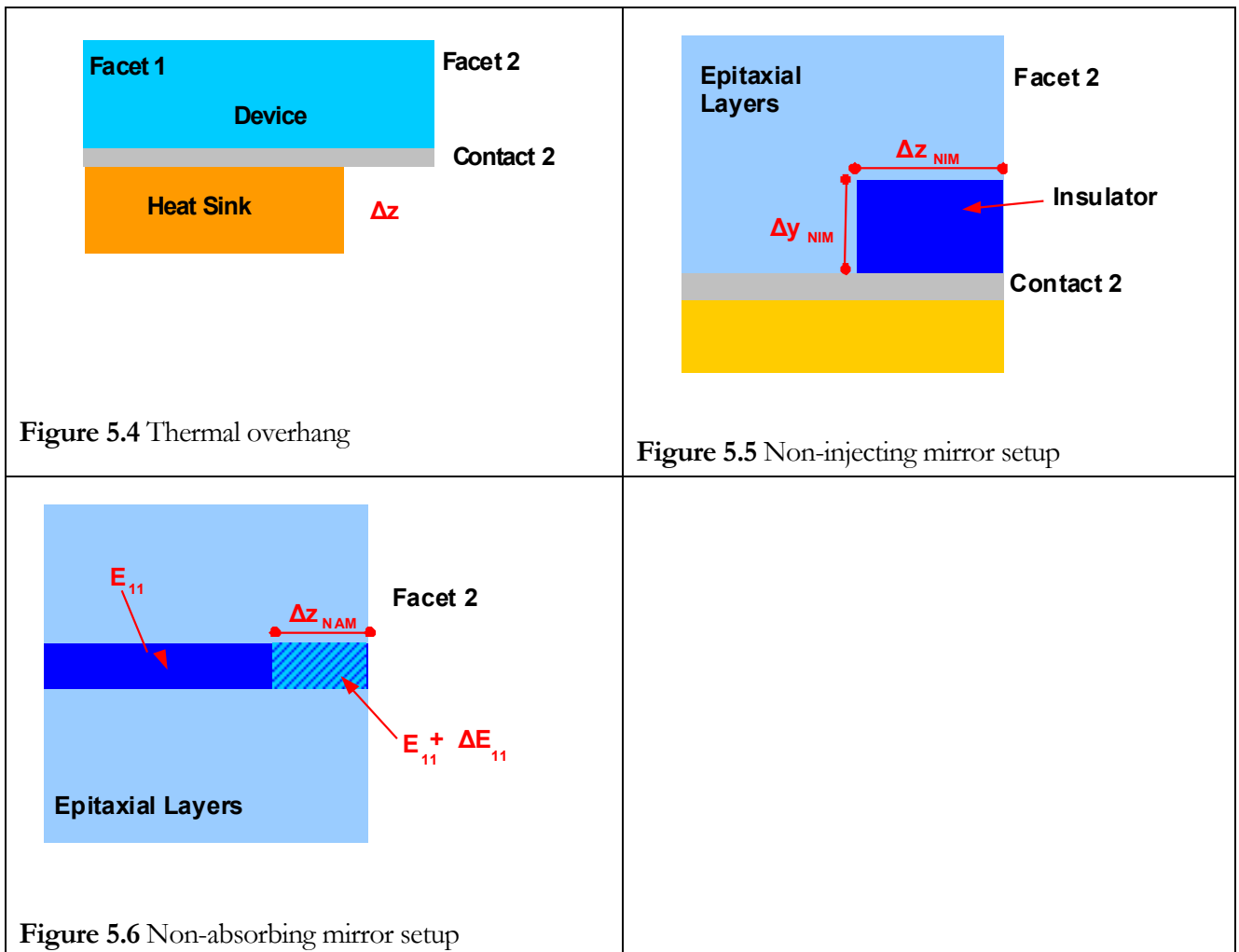
- **Heat Sinks** : press this button to change the device specific properties of the heat sinks. These properties include:

U-Temp	Temperature in ℃ at the device upper boundary (first layer). Default values: 25
U-ThermResist	Thermal resistivity at the device upper boundary (first layer).
U-SeriesThermRes	Thermal resistance at the device upper boundary(first layer).

L-Temp	Temperature in ℃ at the device bottom boundary (last layer). Default values: 25
L-ThermResist	Thermal resistivity at the device bottom boundary (last layer).
L-SeriesThermRes	Thermal resistance at the device bottom boundary (last layer).

5.3   The Simulator

Figure 5.7 shows the *Simulator* dialog. It allows the user to set the control parameters of the simulation – for example the maximum current and the current step. Once the user has set the simulation parameters that they require, the user can press the Start button to start the simulation.

Figure 5.7: The Simulation Panel

At this point, HAROLD will extract all the information it requires to set up and perform the simulation. In the simulation:

- ➢ The Start button will change to Stop indicating that you can cancel the simulation at anytime;
- ➢ The **Bias** progress bar will show the bias progress;
- ➢ The **Z Position** progress bar will show the current z position simulating (2D);
- ➢ The **2D Convergence** progress bar will show the current 2D convergent status (when you are running in 2D mode).

All the parameters of the simulator are listed below:

Device	specifies the name of the device for this simulation
maxStep	Maximum current in *Ampere* reached by the simulation under current bias.
currentStep	Increment of the current from one bias to the next, in *Ampere*. The starting bias current corresponds to the switching voltage.
Running Mode	*One Dimensional* , *Two Dimensional* and *PICWAVE Model* simulation. If you want to generate gain spectra for the last bias, you must select *One Dimensional* simulation and specify the

	wavelength range (**minLamda**, **maxLamda**, and **delLambda**). Select *PICWAVE model* to do a simulation which will generate .swg and .mat files for PicWave.
Execution Mode	*Self-heating*, *Isothermal*, and *Test* mode (find 1D solution at zero voltage and stop).
outputLastBias	Checked to record position dependent quantities (e.g. band edges, fermi levels etc.) for the last simulated bias. If you want to generate the gain or spontaneous spectra, you should check this option.
lockPhotons	(Only 2D) If checked, Harold will not solve the photon balance equation during in the 2D module. Instead, it uses the photon density yielded by the 1D module. Useful for debugging purposes
minLamda	minimum wavelength for the spectra calculation.
maxLamda	maximum wavelength for the spectra calculation.
delLambda	wavelength increment for the spectra calculation.

Pressing the Iteration Parms brings up dialog for setting the following parameters:

maxLongScans	(Only 2D) Maximum number of scans across the longitudinal mesh for iterative solving the photon balance equation and 2D electrical equations. See section 3.2.2. Default value = 5.
maxIterations	Maximum number of Newton-Raphson iterations (see Section 8.4). Default value = 40
maxElecThermalIter	(Only 2D) Maximum number of iterations between 2D electrical solution and 2D thermal solution. Default value = 20
maxRelaxSteps	(Only 2D) Maximum number of relaxation steps used in solving the 2D heat flow equation.
voltageBiasOnly	If TRUE, Harold will iteratively use voltage bias to drive the device to the specified current bias. Otherwise, it will apply current bias to the device directly in the current bias simulation step. You can get more accurate current and avoid the missing of current bias in some cases when you set it true, but with the expenditure of much longer simulation time.
adaptiveBiasStep	If TRUE, Harold will automatically halve the bias step size (either the voltage or current step size) if the Newton-Raphson iteration process does not converge to the required accuracy by the last iteration (see Section 8). Thereafter the bias step size will be increased by 10% whenever convergence is achieved, up to a maximum value given by either the V-Increment or the currentStep defined by the user. This is useful for solving convergence problems resulting from poor initial guess solutions due to too large a bias step.
maxNumBiasTries	(If **adaptiveBiasStep** true) Maximum number of successive bias step reductions allowed in trying to achieve convergence to required accuracy.

displayWarning	If TRUE, Harold will display the warning messages in the simulation. Useful for debugging purpose.
displayResiduals	If TRUE, Harold will display information about the solution process (see Section 8) in the message log. This is useful for identifying and tracing the causes of convergence problems. The maximum residual and maximum normalised correction for the optoelectronic equations (out of all Y-mesh points) are printed for each iteration at each Z-mesh point for each bias. Also printed are the corrections due to bandgap narrowing and self-heating effects (maximum bandgap wavelength change in the QWs and maximum temperature correction out of all T-mesh points, respectively).

Pressing the Numerical Limits brings up dialog for setting the following parameters:

residualLimit	Upper limit for residuals (see Section 8.2). Default value $= 10^{-8}$
numericalLimit	Numerical accuracy of the solution (see Section 8.3). Default value $= 10^{-8}$
clamp	Clamp value for the potentials, in units of kT_0/e (see Section 8.3). Default value $= 5$
tempRes	Accuracy of the temperature, in °C. See Section 8.4. Default value $= 0.1$
lambdaAccuracy	Accuracy of the wavelength, in *nanometers* . See Section 8.4 . Default value $= 0.1$
thermRelaxCutoff	(Only 2D) Temperature cutoff for the relaxation procedure in solving the 2D heat flow equation. The relaxation method stops if the maximum variation of the local temperature at any given 2D mesh point is lower or equal to this value.

Pressing the QWSolver Parms brings up dialog for setting the parameters of series solving the quantum well structures:

mqwCoupled	This parameter is only used for the quantum well definition set you provided. If TRUE, the quantum well set are treated coupled, i.e. Schroedinger's Equation is solved for the whole set of quantum wells, otherwise uncoupled – i.e. Schroedinger's Equation is solved for just one quantum well and the gain is then multiplied by the number of wells.
qwsSelfConsistent	If TRUE, Harold will solve the Poisson and Schrödinger's Equations self consistently for each bias. You can get more accurate results for each bias but with the cost of much longer simulation time.

maxConfinementWidth This controls the amount of the first and last QW barrier layer (*confinement* type layer) that is passed to the Schroedinger Equation solver. Generally you only need 15nm or 20nm of barrier to get a good solution – larger amounts usually just waste spatial resolution. Do a test simulation and check the resulting quantum well wavefunctions are ok i.e. that the wavefunction amplitude and its spatial gradient reach zero before the boundaries but that there is not a large amount of wasted space.

Pressing the PicWAVE Parms brings up *PicWave Model Parms Editor* to set the following parameters for the generation of PicWAVE files:

exportedMatFile The file name for the generated PicWave .mat file.

exportedSwgFile The file name for the generated PicWave .swg file.

INCLUDE-MatFile The file name of included mat file of .mat file

NGmaxNTerms Number of g(N) polygon terms.

nG2Nterms Number of g2(N) polygon terms for polynomial format or values for SPLINEXY format.

NLamPeakNTerms Number of lam_pk(N) polygon terms.

NTempTerms Number of temperature dependence polygon terms.

InterpolationBeforeFit interpolation method before fitting gain related parameters (gain peak, gain curvature, and gain peak position)

minN Minimum carrier density for gain fitting.

maxN Maximum carrier density for gain fitting.

picWaveFreeSpectraRange free spectra range of PicWave .

ignorePeakShiftBelowNo If set to 1, the gain peak position is fixed at the value corresponding to the transparent carrier density; if 0, the gain peak position is set to the first transition wavelength of the quantum well.

minT Minimum temperature for gain calculation.

MaxT Maximum temperature for gain calculation.

g2FitType polynomial or spline format for g2.

g2ClipFactor the maximum g2 is limited by g2ClipFactor* average of g2

maxDeltaRIX Maximum refractive index change for grading layer slice. At present, PicWave can't deal with the graded layer. This parameter is used for controlling how to slicing the graded layer into some slab layers for PicWave. After slicing, the refractive index difference between two neighbour slab layers will not exceed maxDeltaRIX.

gain_eps nonlinear gain(Pass through parameters)

lef	linewidth enhancement factor (Pass through parameters)
rho	electric conductivity (Pass through parameters)

Pressing the `Mesh Parms` brings up dialog for setting up the default mesh steps for each kind of layer.

5.4 Simulation results

Once the simulation has finished, the user can press the `Inspect` button which will display the *Simulation Results* dialog box. (which is shown in **Figure 5.8a** and **Figure 5.8b**). HAROLD generates a lot of data which is broadly split into four categories: *1D Results*, *Test Results*, *2D Results* and *Per Bias Results*. These will now be explained.

- *1D Results*: These are functions of y-position (i.e. functions of the position within the epitaxial layer structure) only and can only be obtained if the simulation was performed using the *One Dimensional* Running Mode. **Note that the origin (O) of these results corresponds to the interface between the substrate and the first core layer nearest the substrate. The results extend to the last core layer. Therefore, results are plotted as a function of core position.**

  The *1D Results* panel also gives a button `Spectra` for you to press it to display the gain/spontaneous spectra results window as shown in **Figure 5.8c**.

  The *1D Results* panel also gives a button `thermal` for you to display extra thermal results as show in **Figure 5.8d**.

- *Test Results*: These are results obtained when the simulation is performed with the *execution mode* set to *Test*. (Test mode does a simulation at zero bias.)

- *2D Results*: These are functions of y and z (i.e. functions of the epitaxial layer position and the longitudinal position in the cavity).

- *Per Bias Results*: These are functions of either the applied voltage, the current or the current density.

- *Quantum Well Wavefunction*: These are the envelope wave functions and their corresponding eigenvalues(energy levels) of quantum well structures.

The 1*D Results*, *Test Results* and *Per Bias Results* panels work in a similar way. You can set the x-axis plotting range and the number of points. You then have the choice of plotting a single graph by clicking on one of the lines in the "Available Plots" list and pressing the `Plot` button next to this list. Alternatively, you can also plot several functions on the same chart. To do this, simply select a line in the "Available Plots" list and press the `==>` button. You will see the same line appear in the "Multiple Plots" list. Once you have finished moving the desired functions into the "Multiple Plots" list, simply press the `Plot` button next to the list. If you make a mistake, hilight the line you wish to remove from the "Multiple Plots" list and press the `<==` button.

5.4.1 Test Results

The Results panel for *Test Execution Mode* is shown above. The *Test Execution Mode* will allow you to plot the information given in the list below, each quantity being plotted as a function of y (the vertical coordinate).
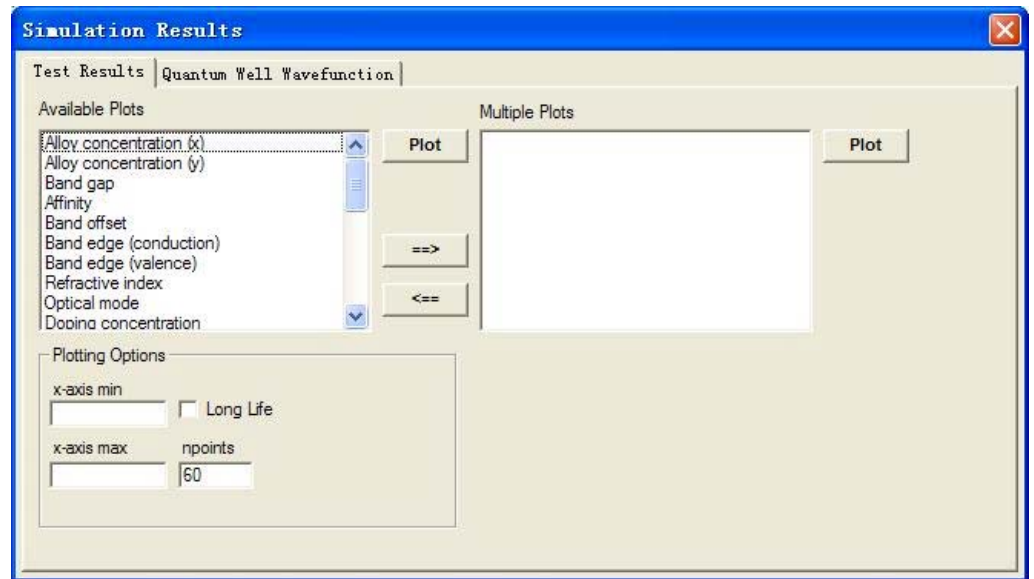
Figure 5.8a: The Simulation Results Dialog box for Test Execution Mode

- Alloy concentration (x)
- Alloy concentration (y)
- Band gap
- Affinity
- Band offset
- Band edge (conduction)
- Band edge (valence)
- Refractive index
- Optical mode
- Doping concentration
- Intrinsic carrier density
- Effective electron bulk mass
- Effective hole bulk mass
- Electron density of states
- Hole density of states
- Relative permittivity
- Electron diffusivity
- Hole diffusivity
- Electron mobililty
- Hole mobility

- Electron Auger coefficient
- Hole Auger coefficient
- Free electron absorption coefficient
- Free hole absorption coefficient

5.4.2 One Dimensional Execution Mode
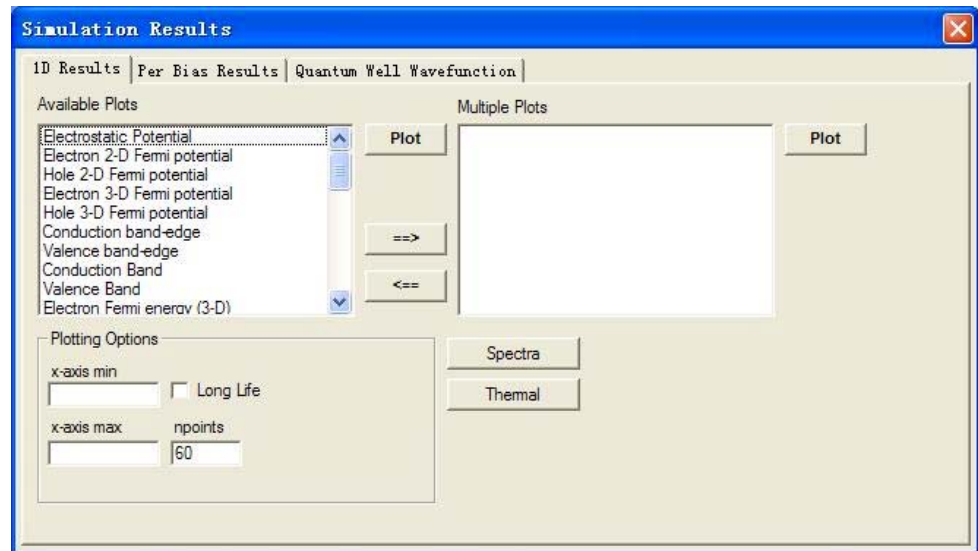
Figure 5.8b: The Simulation Results Dialog box for One Dimensional Execution Mode

Available plots for *One Dimensional Execution Mode* are list below:

- Electrostatic potential
- Electron 2D Fermi potential
- Hole 2D Fermi potential
- Electron 3D Fermi potential
- Hole 3D Fermi potential
- Conduction band edge
- Valence band edge
- Conduction band
- Valence band
- Electron Fermi energy (3D)
- Hole Fermi energy (3D)
- Electric field
- Electron density (qw)
- Hole density (qw)
- Electron density (bulk)
- Hole density (bulk)

- Total charge
- Electron current density
- Hole current density
- Total current density
- SRH recombination (bulk)
- Spontaneous recombination (bulk)
- Auger recombination (bulk)
- Net recombination (electrons)
- Net recombination (holes)
- SRH recombination (qw)
- Spontaneous recombination (qw)
- Auger recombination (qw)
- Stimulated recombination
- Averaged gain
- Temperature

As well as the information in the table above, the *1D Results* panel also gives a button Spectra for you to pressing it to display the gain/spontaneous *Spectra Results* window as shown in **Figure 5.8c**.
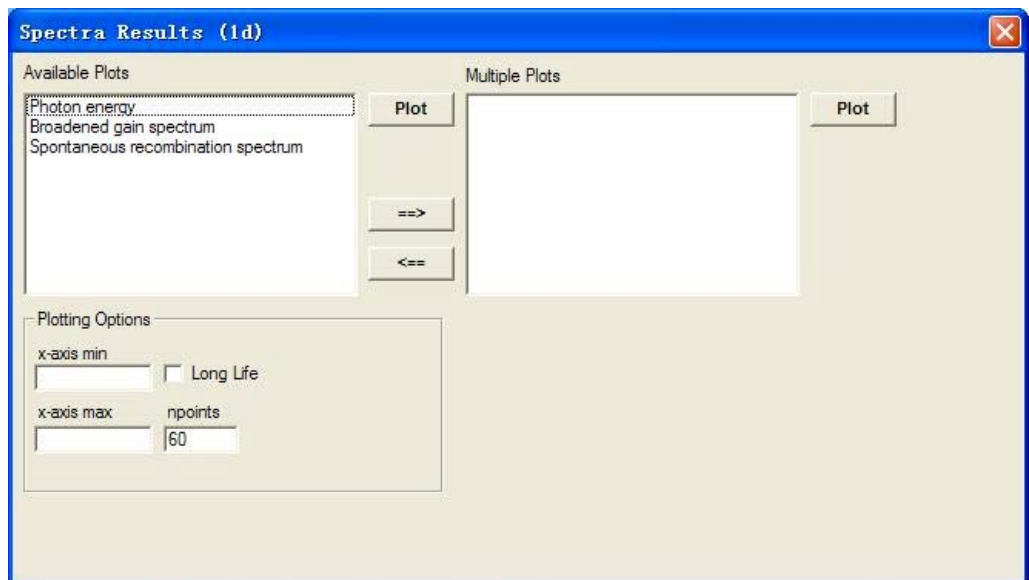
Figure 5.8c The Spectra Results panel for 1d simulation

The *1D Results* panel also gives a button Thermal for you to display extra thermal results as show in **Figure 5.8d**.
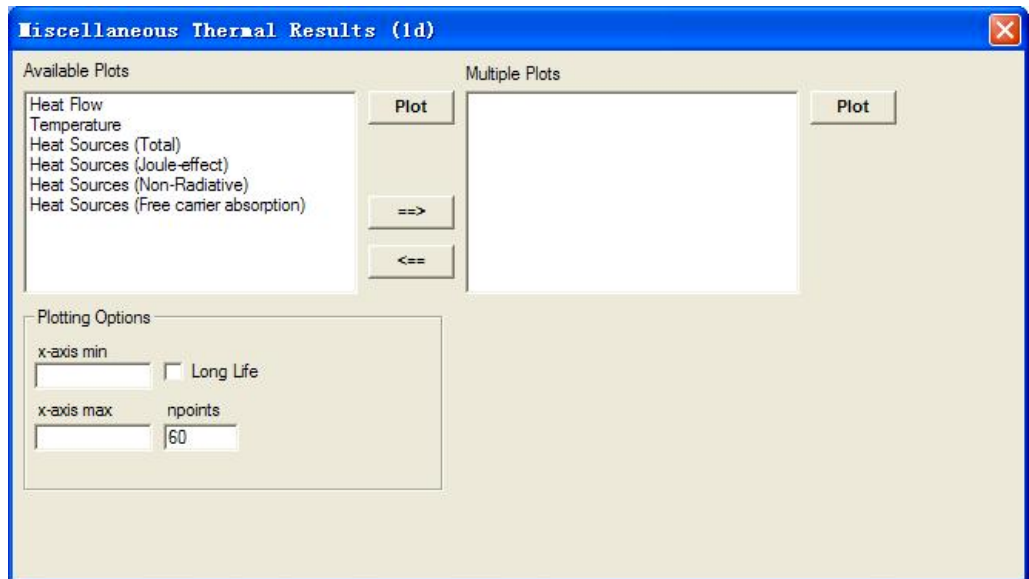
Figure 5.8d: The Miscellaneous Thermal Results panel for 1d simulation

5.4.3 Two Dimensional Execution Mode

The *2D Results* panel works in a slightly different manner. **Figure 5.9** shows the *2D Results* panel. The *2D Results* are split into 6 sub-categories:

- **Bands**

- **Carriers**

- **Currents**

- **Thermal**

- **Quantum Well**

- **Spontaneous Emission**
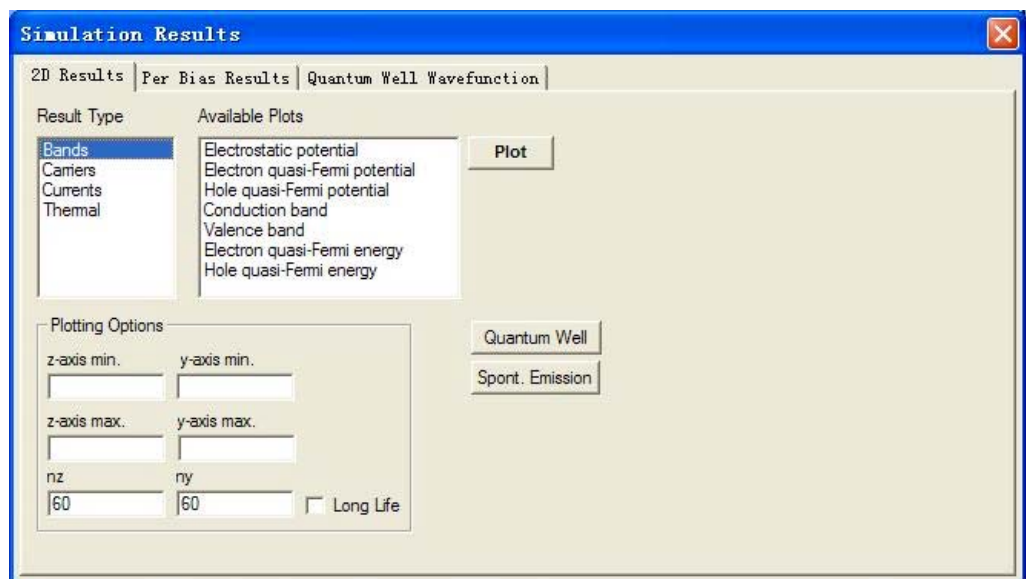
Figure 5.9: The *2D Results* panel

5.5   The trap definintion set edtior

Figure 5. 10 shows the *Trap Definition Set Editor*. Use the `New` button to add a trap, `Cut` button to delete and copy selected trap to clipboard, `Copy` button to copy selected trap to clipboard, `Paste` button to paste a trap from the clipboard. Press `Accept` button to save the results into the project.
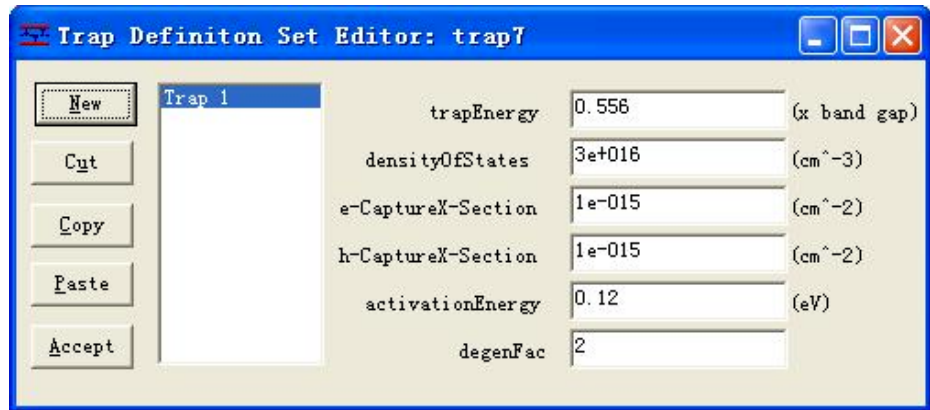
Figure 5. 10 The Trap Definition Set Editor

trapEnergy	Energy level of the k-th *trap* E_k, eq. (3-31). The value must be given in units of the band gap energy. For example, the value 1 specifies a trap located exactly at the conduction band, while the value 0, at the valence band.
densityOfStates	Density of states N_k for the k-th trap level, eqs. (3-32) and (3-33) , in cm^{-3}.
e-CaptureXSection	Electron capture cross section corresponding to the k-th trap level at room temperature σ_{nk}^0, eq. (3-34), in cm^{-2}.
h-CaptureXSection	Hole capture cross section corresponding to the k-th trap level at room temperature σ_{pk}^0, eq.(3-35), in cm^{-2}.
activationEnergy	Activation energy of the k-th trap level E_{ak}, eqs. (3-34) and (3-35), in eV.
degenFac	Degeneracy factor for the k-th trap level g_k, eq. (3-31).

5.6　The quantum well levels set editor

Figure 5.11 shows the *Quantum Well Set Editor.* Use the New button to add a quantum well, Cut button to delete and copy selected quantum well to clipboard, Copy button to copy selected quantum well to clipboard, Paste button to paste a quantum well from the clipboard. Press Accept button to save the results in to the project.

Click Condution Band , Light Hole Band or Heavy Hole Band button for each band and brings up the *Level Definition Editor* as shown in **Figure 5.12**. The operation of level editor is similar to the *Quantum Well Set Editor*.
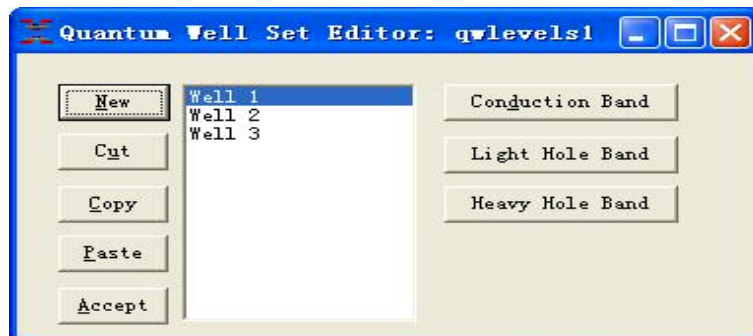
Figure 5.11　The Quantum Well Set Editor
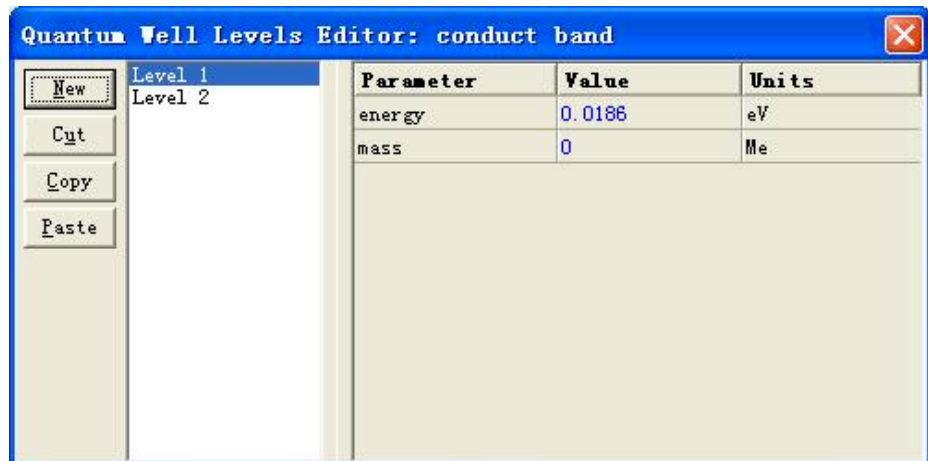
Figure 5.12　The Quantum Well Levels Editor

energy　　　　　　　Energy of the level in eV, relative to the bottom of the band.

mass　　　　　　　Effective mass associated to the level, in unit of the electron rest mass. If this parameter is left blank, the mass will be calculated from the parameters of the material database, according to the layer material and composition.

5.7 The Mesh Policy Editor

Figure 5.13 shows the *Mesh Policy Editor*, the operation of it is similar to the *Trap Definition Set Editor*.
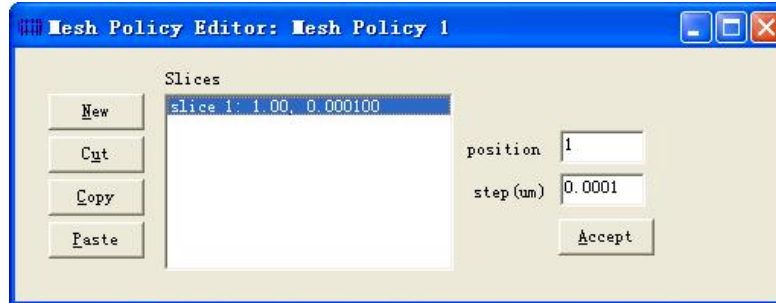
Figure 5.13 The Mesh Policy Editor

position   relative position of each slice to the edge of a layer

step   mesh step in each slice.

5.8 The application setting dialog

In the main window of the application, selecting Options->Setting will bring up the application settings dialog as shown in following figure. You can set the material files location for the application.
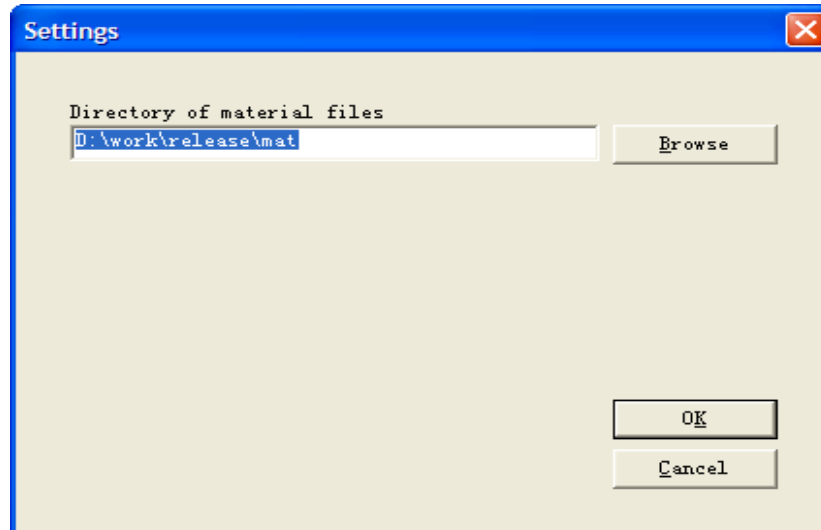
5.9 The PicWave Results Panel

After running a *PicWave Model* simulation and pressing the [Inspect] button, the PicWave results panel will pop up as show in the screen-shot below.
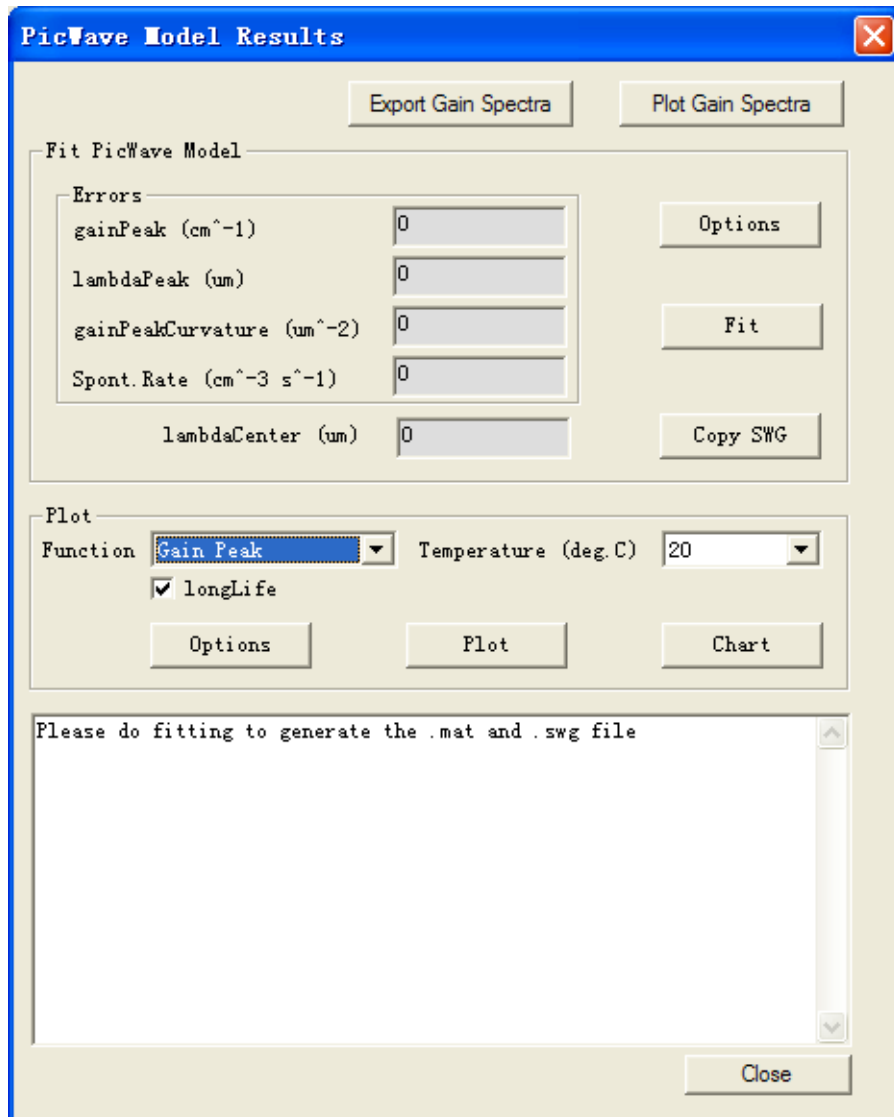
Export Gain Spectra	Export all gain spectra during the simulation.
Plot Gain Spectra	Plot all gain spectra during the simulation.
Options	the same parameters as those pressing Simulator-> PicWave Parms .
Fit	press it to generate the PicWave files.
Copy SWG	copy the .swg file into the clipboard.
Plot|Function	select which function to plot.
Plot|Temperature	select the temperature at which the function to plot.
Plot|Options	plot options.
Plot|Plot	plot the selected function.
Plot|Chart	plot chart for exporting data.

Chapter

6

PicWave Link

Harold now can automatically generate data files for PicWave. Harold can model the detailed physics of a quantum well structure but is restricted to relatively simple device structures – typically just a Fabry-Perot cavity. In contrast PicWave can model very complex devices including DFB and tuneable devices. However it does not have the ability to compute gain functions from a detailed description of the quantum well structure – it starts with a set of "material functions" describing e.g. the gain versus carrier density dependence. Harold's PicWave link allows you to do a detailed material simulation and import the results of this into PicWave. This gives you the best of both worlds – a detailed drift-diffusion quantum mechanical model of the electronic structure, and a flexible device model. It also has the benefit of allowing the device model to run at high speed since the material functions generated by Harold can be evaluated very quickly.

The link works by generating two files – a ".mat" file, containing a description of a special material that reproduces the Harold-computed results, and a ".swg" (slab-waveguide) file, which describes the epitaxial structure that you defined in Harold, described in a way that can be read by PicWave.

The PicWave Link can also be used to export materials to CLADISS-2D. However CLADISS-2D support will be removed in future versions of Harold

This chapter will describe the process of creating a PicWave model.

6.1   Generating a PicWave model

First ensure that your Harold device is operating as desired. Then:

- Enable the Link by setting **Running Mode** to *PicWave Model* on the Simulator Panel and then .

- Click the PicWave Parms button and set the parameters as desired – these are described below.

- Ensure that the Spectrum Generator parameters (minLambda, maxLambda, delLambda) are set to give a spectrum covering all areas of interest and at a good wavelength resolution – a resolution of 2 nm is a good starting value.

- Ensure the current range and step are appropriate. You will want to generate a current scan with perhaps 50 or so points in it. You may need to alter this after doing an initial Link simulation.)

- Press the Start button.

This will begin a special Harold simulation which turns off the cavity mirrors so that the laser does not reach threshold. The simulation will record the gain and

spontaneous emission spectra at each current step and will use these data to create a fitted model. Once the simulation is finished, click the $\boxed{\text{Inspect}}$ button. The *PicWave Results* panel shown below will appear.

PicWave Results Panel: from here you can inspect the quality of the fitting, plotting the computed and fitted functions.

From this plot you can inspect the results of the fitting process, including:

- gain peak versus carrier density – comparing the computed gain peak function with the fitted (polynomial) function.

- Gain peak wavelength versus carrier density

- Gain peak curvature versus carrier density

- Spontaneous emission rate versus carrier density

All these functions have been computed at one or more temperature – choose the temperature that you desire with the control supplied.

In addition you can plot a Stacked Gain Spectrum Plot – containing all the computed and fitted spectra on one plot.

We strongly recommend that you view all these plots every time that you export a PicWave model, to ensure that the fitting has run properly.

Things to check for when generating a PicWave Model

1. the gain spectrum will go multi-peaked at high carrier density, as higher quantum well states are populated. PicWave only supports one gain peak so the peak wavelength will jump suddenly when the next quantum state provides more gain than the first one. This is likely to generate a poor LambdaPeak vs. carrier density fit. Check the Stacked Gain Plot and LambdaPeak plot, and if you see that a wavelength jump has occurred then try increasing **nLamPeakNTerms**. If this still does not help, then you will need to run the model simulation to a carrier density below the wavelength jump (i.e. decrease **maxN**).

2. Check the computed and fitted GainPeak function – are they well matched? If not, try doing another fit with a different **nGmaxNTerms** value.

3. If you do a fitting to too few points (large current-step) you can easily get silly polynomial functions e.g. the computed function is not smooth This is illustrated in the figure below.

Fitted function goes below zero

Computed points
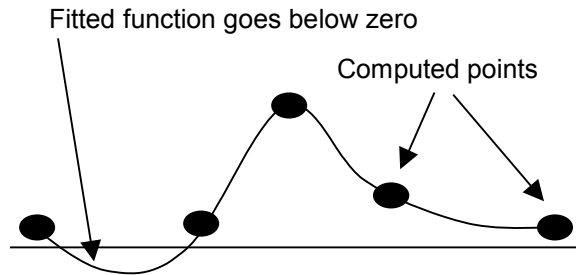
The usual cause of such behaviour is a too-large current step and the solution is to set "Current-step" to something smaller and re-do the PicWave Model simulation.

6.2   Importing Model to PicWave

Harold will provide two sets of data to PicWave:

  a) a set of epitaxial layers (swg structure)
  b) a material file (.mat) with one or more materials describing the materials of the swg structure.

The names of these materials are all of the form "HRDxxxxx" so that you can easily identify them as Harold-generated. The names of the .mat and .swg files are set in the *PicWave Model Parms Editor* before you run the fit. The generated .mat file will also reference an existing .mat file so that you can use additional non-Harold generated materials in your PicWave waveguide. To define the name of this .mat file, enter its name in the **INCLUDE-MatFile** property of the *PicWave Model Parms Editor*.

Once you have ensured that you have a good fit to the simulated results, you are ready to import the model to PicWave. Remember that PicWave can simulate a much more complex geometry than Harold can. The procedure below assumes that you will generate a PicWave device "from scratch".

➢ From PicWave create a new project.

➢ In the new project, create a new *Device* and name it "hrldDevice"

➢ In the new project, create a new *RWG Waveguide* and name it "hrldWG"

➢ In the new project, create a new *Time Domain Calculator* and name it "hrldCalculator"

➢ Save the project to the directory that Harold wrote the .mat file (or else copy the .mat file to wherever you save the new project.

➢ Display "hrldWG" (double-click on its node in the project tree.)

➢ Open the RWG Editor (/Edit/Waveguide).

➢ Set the material database to the .mat file generated by Harold.

➢ Switch back to Harold

➢ Click on the `Copy SWG` button to copy the epitaxy layer structure to the clipboard.

➢ Switch back to the RWG Editor in PicWave

➢ Click the `New Slice` button.

SWG Manager ☒ Local SWGs cl2d_example1.swg New | Delete | Copy | Paste Close **Above**: Harold-generated swg pasted into SWG-Manager	➢ Click the Paste button to paste the Harold-generated swg into the SWG list ➢ The Harold-generated .swg should now appear in the list (see left). ➢ Select the new swg in the list so that it is highlighted ➢ Click the Close button. This will return you to the RWG Editor and you should see that the RWG now has one slice, referencing the new swg. ➢

➢ You must now decide what lateral structure to give your waveguide – remember that Harold did not take any account of the lateral structure. We will assume for now that you wish to recreate exactly the Harold simulation in PicWave and so that you do not want to add any lateral structure.

➢ Set the width of the slice to the same width of the Harold "cavity" parameter "width".

➢ Set the LHS and RHS boundary conditions to "electric wall".

➢ Set the rwg's WG Solver Parms wavelength to the **lambdaCenter** value reported in Harold's PicWave Results panel.

➢ Display the "hrldDevice".

➢ Add a new Section to the device

➢ Set the following properties of the Section:

- **wgName** to "hrldWG"

- **length** to match that in your Harold simulation

- **nCellW** = 1

- **activeType** = "*gain*"

Next you must add an electrical connection to *each active layer* in the swg:

➢ Click on the Current Flow Model property to edit it.

➢ Another editor will appear, click on the **alConnections** property to display the **alConnections** editor. Click New button to create a new connection. Set the resistivity to 1 ohm.um2 (a reasonable default unless you know a better value).

➢ Add further connections for each additional active-layer in the swg structure (an active layer is a layer in the SWG structure that has the "isActive" flag set) and will be coloured in red in the RWG Waveguide window.

➢ Edit the Device properties (/Edit/Device Properties) and set the facet reflectivities to whatever they were in your Harold simulation.

➢ Add one Contact to the Device from the Contacts property, and set the contact's start and end width as desired.

➢ Display the *hrldCalculator* you created earlier.

➢ In the Control panel of the Calculator, set **lambdaCenter** to the value that was reported in Harold's *PicWave Results* panel.

> In the "Main" panel of the Calculator, set **zstep** to a value equal to or less that the value reported in Harold's *PicWave Results* panel.

You should now set up all the other parameters as per any other PicWave simulation – add a set of instruments and add a Drive Signal for the electrical contact.

6.3   The PicWave Model – Technical Details

This chapter describes the details of the model exported to PicWave. Harold exports the following quantities:

- peak gain gpk(N,T)
- wavelength of gain peak lpk(N,T)
- curvature at gain peak – $d^2g/d\lambda^2$(N,T)
- refractive index n(x,y,T, λ)
- bandgap Eg(x,y,N,T)

6.3.1   The gain model

The material gain is given by

$$g = g_p(N,T) - G_0 N_0 g2(N,T)[\lambda - \lambda_p(N,T)]^2 \text{ in units of 1/cm.}$$

This function is constructed by the g_p, g2 λ_p models described below. The gain spectra is modelled in PicWave by the Lorentzian shape function:

$$g(\lambda) = g_p / [(1 + \tau^2(\lambda^{-1} - \lambda_p^{-1})]^{1/2}.$$

For a given carrier density N, the gain spectra is calculated by Harold and then fitted into the above shape to obtain the primitives $g_p, \lambda_p,$ and τ. The relationship between g_2 and τ is

$$g_2 = 0.5\tau^2 / \lambda_p^4.$$

It should be noted that:

> λ_p is fixed at the band edge or at the wavelength corresponding to the transparent carrier density when the carrier density is below transparency.

> The maximum τ is limited by $\tau_{max} = \lambda_p^2 / \Delta\lambda_{min}$. You can also control the minimum τ via the PicWave Model parameters – this is useful otherwise the curvature will go very high near transparency, making a good polynomial fitting difficult.

6.3.2   The gain peak model

The gain peak is modelled by

$$g_p(N,T) = \sum_{i=0}^{nT-1}\sum_{j=0}^{nN-1} c_{ij}(T-T_0)^i(N/N_0)^j$$

where N_0 is the transparent carrier density at the reference temperature T_0.

The units of g_p, Go, No, T are cm^{-1}, cm^2, cm^{-3} and ^oC respectively. This function is written to the .mat file as the GAINL_POLYNT parameter. See PicWave documentation for full details.

6.3.3 The gain peak curvature model

The curvature of the gain peak is modelled by

$$g2(N,T) = \sum_{i=0}^{t} \sum_{j=0}^{n} c_{ij}(T-T_0)^i(N/N_0-1)^j .$$

$g2$ is in unit of μm^{-2}. This function is written to the .mat file as the GAIN_CURVNT parameter. See PicWave documentation for full details.

6.3.4 1.4 The wavelength peak model

The wavelength corresponding to the gain peak is modelled by

$$\lambda_p(N,T) = \sum_{i=0}^{t} \sum_{j=0}^{n} c_{ij}(T-T_0)^i(N/N_0-1)^j$$

This function is written to the .mat file as the GAIN_LAMNT parameter. See PicWave documentation for full details.

6.3.5 Gain Calculation

The gain spectra is modelled by the Lorentzian shape function

$$g(\lambda) = g_p /[(1+\tau^2(\lambda^{-1}-\lambda_p^{-1})]^{1/2} .$$

For a given carrier density N, the gain spectra is calculated by Harold and then fitted into the above shape to obtain the primitives $g_p, \lambda_p,$ and τ. The relationship between g_2 and τ is

$$g_2 = 0.5\tau^2/\lambda_p^4 .$$

It should be noted that:

➢ λ_p is fixed at the band edge or at the wavelength corresponding to the transparent carrier density when the carrier density is below transparency.

➢ The maximum τ is limited by $\tau_{max} = \lambda_p^2/\Delta\lambda_{min}$

6.3.6 The refractive index model

The refractive index is modelled by

$$n(x,y,T,\lambda) = RIX\_FUNCXY(x,y) + RIX\_POLYT(T) + RIX\_POLYL(\lambda)$$

with

$$RIX\_FUNCXY(x, y) = \sum_{i=0}^{nx} \sum_{j=0}^{ny} a_{ij} x^i y^j \quad \text{(polynomial form)}$$

$$RIX\_POLYT(T) = \sum_{i=0}^{nT} b_i (T - T_0)^i$$

$$RIX\_POLYL(\lambda) = \sum_{i=0}^{n\lambda} c_i (\lambda - \lambda_0)^i$$

The material loss has the same model as that of the refractive index.

6.3.7 The bandgap model

The bandgap is modelled by:

$$Eg(x, y, T, N) = EGAP\_FUNCXY(x, y) + EGAP\_POLYT(T) + EGAP\_POLYN(Ne)$$

with

$$EGAP\_FUNCXY(x, y) = \sum_{i=0}^{nx} \sum_{j=0}^{ny} a_{ij} x^i y^j \quad \text{(polynomial form)}$$

$$EGAP\_POLYT(T) = \sum_{i=0}^{nT} b_i (T - T_0)^i$$

$$EGAP\_POLYN(N) = c(N / N_0)^{1/3}$$

Eg is in unit of eV.

6.3.8 The diffusion coefficient model

The diffusion coefficient is described by

$$D(x, y, T, N) = DIFFUSE\_FUNCXY(x, y) + DIFFUSE\_POLYT(T) + DIFFUSE\_POLYN(N)$$

with

$$DIFFUSE\_FUNCXY(x, y) = \sum_{i=0}^{nx} \sum_{j=0}^{ny} a_{ij} x^i y^j \quad \text{(polynomial form)}$$

$$DIFFUSE\_POLYT(T) = \sum_{i=0}^{nT} b_i (T - T_0)^i$$

$$DIFFUSE\_POLYN(N) = \sum_{i=0}^{nN} c_i (N / N_0)^i$$

The unit is cm^2/s .

Chapter

7

Material Database

When you specify a material for a given layer, HAROLD will look for a file in a "Materials" directory with a filename *identical* to that which you have specified as the name of the material. Thus, if you write "mymaterial" the file "mymaterial" must exist in the Materials directory. If the file exists it will read its contents and use the information to build the quantities it needs to carry on the simulation.

Harold looks for the Materials directory as follows:

a) it first looks in the directory of the project that you are running

b) it then looks in the application Materials directory – you can set this from the application's /Options/Setting menu.

We recommend you keep a central Materials directory that you use with all your projects but sometimes you may wish to use a different one for a particular calculation – then put one in the project directory.

Upon installation you will find a Materials directory under Examples. This contains descriptions for common materials but you may build up your own materials data by reference to the syntax described below.

7.1   Supplied Data

Harold comes supplied with data for the following materials:

Al(x)Ga(1-x)As on GaAs

Al(x)Ga(y)In(1-x-y)As grown on GaAs

In(1-x)Ga(x)As(1-y)P(y) grown on GaAs

In(1-x)Ga(x)As(y)P(1-y) grown on GaAs (lattice matched)

In(1-x-y)Ga(Y)Al(X)As grown on InP

In(1-x)Ga(x)As(1-y)P(y) grown on InP

All data contained in these files has been obtained from published journals. The data is only as accurate as the data obtained from these sources and we make no guarantee for its validity. For any highly critical use, you should check all parameters yourself to ensure that they are suitable for your situation.

You are encouraged to modify the supplied materials as more reliable data becomes available in the literature. You can also create completely new Harold materials by reference to this Chapter. Useful sources of data on the Internet may be:

Ioffe Institute: www.ioffe.rssi.ru/SVA/NSM/Semicond/

Purdue University:

 http://yara.ecn.purdue.edu/%7Emslhub/MaterialsDBase/frames.html

NUSOD: www.nusod.org

7.2   Database syntax

Entries into the material database have the following general form (the numbers at the right are only to guide the reader and should not be included into the actual database):

'Identifier'	*1*
'Function'	*2*
Number_of_segments	*3*
x1,x2	*4*
y1,y2	*5*
Number_of_parameters_per_line, Number_of_lines	*6*
Parameters	*7*
...	
...	
'Thermal_model'	
Number_of_parameters	
Parameters	

The first line is for the *Identifier* which specifies the particular quantity (*e.g.* [GAP]), while *Function* tells the program which functional form, *f (x,y)* , has to be used to calculate such quantity. In general, the domain of the function are the alloy concentrations, *x* and *y* , where $0 \leq x \leq 1$, $0 \leq y \leq 1$. HAROLD, allows the possibility to split the function arguments in various segments, such that different parameters can be specified for regions with different properties. Accordingly, the third line specifies the number of segments in which the given function has been split. The following lines 4-7 are related to the particular segment. Lines 4 and 5 specify the range of variation of the alloy concentration. Line 6 specifies the number of parameters given on each line below, and the number of subsequent lines the program should read. The actual parameters are specified in line 7 (and possibly next lines).

The structure of lines 4-7 has to be repeated for each segment of the function.

The specification of the parameters depends on the functional form. This topic will be explained in the next section.

The last three lines specified the thermal model. Here, the name of the model must be supplied (usually, either 'THERMAL' or 'ISOTHERMAL', the number of parameters involved followed by the parameters. If 'ISOTHERMAL' is used the number of parameters may be set to 0 so the last line can be omitted.

As an example, let us consider the following parameterization of the band gap:

$$E_g\left(x,y\right)=\begin{cases}1.424+1.247x & 0 \leq x \leq 0.45 & 0 \leq y \leq 1 \\ 1.9+0.125x+0.143x^2 & 0.45 \leq x \leq 1 & 0 \leq y \leq 1\end{cases}$$

this should be written into the material database as,

```
'[GAP]'
'POLY'
2,
0,0.45,
0,1,
2,1
1.424,1.247,
0.45, 1,
0,1,
3,1,
1.9,0.125,0.143
```

Finally, there are certain parameters (like the bulk radiative constant, B) which do not depend at all on the alloy concentration. They are considered as constant functions and simply introduced as,

'Identifier'
Value

For example,

'[RADIATIVE_CONSTANT]'
1.5e-10

Comments

Comments may be inserted in the material database files before, between or after each property definition. E.g. in the bandgap definition above, before the line '[GAP]' or after the line '**1.9,0.125,0.143'.** The comments have no particular syntax.

7.3   Functions

Version 3.0 supports the following functions.

7.3.1   Polynomial

Name : POLY

$$Q(x, y) = \sum_{i=1}^{N_y} \sum_{j=1}^{Nx} C_{ij} x^{j-1} y^{i-1} \qquad N_x, N_y \leq 9$$

Syntax:

$$N_x, N_y$$
$$C_{11}, C_{12}, ..., C_{1N_x},$$
$$C_{21}, C_{22}, ..., C_{2N_x},$$
$$...$$
$$C_{N_y1}, C_{N_y2}, ..., C_{N_yN_x},$$

7-68

Example:

$$Eg(x, y) = 0.361 + 0.676x + 0.751y + 0.384x^2 + 1.658xy + 0.242y^2 - 1.271x^2y - 1.667xy^2 + 1.61x^2y^2$$

'[GAP]'
'POLY'
1,
0,1
0,1
3,3
0.361,0.676,0.384,
0.751,1.658,-1.271,
0.242,-1.667,1.610,

7.3.2 Power Polynomial

Name : POWPOLY

$$Q(x, y) = A_0 B^{P(x,y)}$$

$$P(x, y) = \sum_{i=0}^{N_y} \sum_{j=0}^{Nx} C_{ij} x^j y^i \qquad N_x, N_y \leq 8$$

Syntax:

$$N_x, N_y + 1,$$
$$A_0, B, 0,...,0,$$
$$C_{11}, C_{12}, C_{13},..., C_{1N_x},$$
$$C_{21}, C_{22}, C_{23},..., C_{2N_x},$$
$$...$$
$$C_{N_y 1}, C_{N_y 2}, C_{N_y 3},..., C_{N_y N_x},$$

7.3.3 Vegard

Name : 'VEGARD'
Mode: 1

$$A_x B_{1-x} C_y D_{1-y} : \quad Q(x, y) = \frac{x(1-x)[yT_{ABC}(x) + (1-y)T_{ABD}(x)]}{x(1-x) + y(1-y)}$$
$$+ \frac{y(1-y)[xT_{ACD}(y) + (1-x)T_{BCD}(y)]}{x(1-x) + y(1-y)}$$

$$AB_x C_{1-x} : \quad T_{ABC}(x) = xT_{AB} + yT_{AC} - x(1-x)U_{ABC}$$

Syntax:

4,1,

$T_{AC}, T_{BC}, T_{AD}, T_{BD},$

$U_{ABC}, U_{ABD}, U_{ACD}, U_{BCD},$

Mode: 2

$$AB_xC_{1-x}D_{1-x-y}: \quad Q(x,y) \quad = xT_{AB} + yT_{AC} + (1-x-y)T_{AD} - xyU_{ABC}$$
$$- x(1-x-y)U_{ABD} - y(1-x-y)U_{ACD}$$

Syntax:

3,2,

$T_{AB}, T_{AC}, T_{AD},$

$U_{ABC}, U_{ABD}, U_{ACD},$

7.3.4 Kokubo

Name: KOKUBO

$$Q(x,E) = P(x,E) + \frac{c}{[E+a+bx]^2 + d}$$

$$P(x,E) = \sum_{i=0}^{N_y} \sum_{j=0}^{Nx} C_{ij} x^j E^i \qquad N_x, N_y \le 7$$

Syntax:

$N_x, N_y + 2,$

$C_{11}, C_{12}, C_{13}, ..., C_{1N_x},$

$C_{21}, C_{22}, C_{23}, ..., C_{2N_x},$

...

$C_{N_y 1}, C_{N_y 2}, C_{N_y 3}, ..., C_{N_y N_x},$

$a, b, 0, ..., 0,$

$c, d, 0, ..., 0,$

7.3.5 Doping

Name: DOPING

$$\mu = \mu_1 + \frac{(\mu_2 - \mu_1)}{1 + \left(\dfrac{N_D + N_A}{N_r}\right)^\alpha}$$

where μ_1 and μ_2 are the values of the minimum and maximum mobilities for either electrons or holes.

Syntax:

2,1,

$N_r, \alpha,$

7.4 Parameters

The following parameters might be specified in the material database.

7.4.1 Alloy Composition

You can specify the name for the alloy compositions x and y. Also their relationship can be specified in the material files. The format for x is :

'[COMPOSITION_X]'

'Name'

DependentType

Functions

'Name' is the name for the composition. For example , for AlxGa1-xAs material, . Name should be 'Al'. When it is 'NONE', there is no such alloy composition.

DependentType: 0 when the user can input this on the GUI

1 when x is a function of y: x = F1(y)

2 when x is a function of y: x = F1(y)/F2(y)

Functions: F1(y) and F2(y) when DependentType is not 0. F1(y) and F2(y) can be any of the above function types. Each function should be followed by:

'ISOTHERMAL'
 0,

The alloy composition y has the same format as that of x.

The functions are useful when you want Harold to calculate the mole composition x for y or vice versa for a lattice-matched material.

7.4.2 Energy gap

Symbol: $E_g(x, y)$

Units: eV

Identifier: [GAP]

Functional dependence: POLY

Temperature dependence: THERMAL

7.4.3 Electron affinity

Symbol: $\chi(x, y)$

Units: eV

Identifier: [AFFINITY]

Functional dependence: POLY

Temperature dependence: THERMAL

The electron affinity is, in general, the energy difference between the vacuum level and the semiconductor conduction band (see any basic book on semiconductor device, for instance Physics of Semiconductor Devices, S. M. Sze, Wiley). It is necessary for a correct band alignment of different materials in the case of heterojunctions, as the affinity difference corresponds to the offset of the conduction bands. But unfortunately it is not a well-known parameter for most materials, and in consequence only affinity differences have to be considered.

HAROLD uses the affinity in the following way, similar to that used in the numerical simulation of other heterostructure devices (see Lundstrom and Schuelke, "Numerical analysis of heterostructure semiconductor devices, IEEE Trans Electr Dev, vol ED-30, pp 1151-1159, 1983):

In Chapter 3, χ is the affinity of the material and χ_r is a reference value common for all materials in the device. χ_r should be zero, if the data were well known, but its value is irrelevant if the affinity of all materials in the same device are given using the same reference value. The conduction band alignment of different materials is performed using the affinity value defined here assuming $\chi_r = 0$. In the case of heterojunctions of a single alloy with different compositions (GaAs/Al0.20Ga0.80As, for instance), the value of the reference χ_r is irrelevant, as only affinity differences are important. If a heterojunction is composed of completely different material (GaAs and InP, for instance) it is very important to check that the values of the affinities result in an appropriate alignment of the heterojunction. The expressions in this manual use (χ _ χ_r) instead of χ to point out that the reference value should be consistent between materials to provide proper band alignment. In the literature it is possible to find the conduction band offset in heterojunctions, defined as $\Delta E_c / \Delta E_g$. However, the variation of affinity with composition and temperature is not reported. The affinity in Harold databases is built to provide a known value for the band offset; for instance the band offset in AlGaAs/ AlGaAs heterojunctions is 0.6, and the parameterisation of the affinity yields approximately this value. The above can be better understood after running the code for a given structure in test mode. The output graphs provide at each mesh point the affinity value in database, the band offset for this alloy, and the conduction band edge, which is (minus affinity), prior to solving the Poisson equation and including the electrostatic potential.

7.4.4 Relative static permitivity

Symbol: $\varepsilon_d(x, y)$

Units: ε_0

Identifier: [PERMITIVITY]

Functional dependence: POLY

Temperature dependence: ISOTHERMAL

7.4.5 Refractive index

Symbol: $n(x, y)$ or $n(x, E)$

Identifier: [REFRACTIVE_INDEX]

Functional dependence: POLY - for $n(x, y)$, KOKUBO - for $n(x, E)$

Temperature dependence: THERMAL

7.4.6 Thermal resistivity

Symbol: $\rho_{th}(x, y)$

Units: $°CcmW^{-1}$

Identifier: [THERMAL_RESISTIVITY]

Functional dependence: POLY

Temperature dependence: THERMAL

7.4.7 Relative effective electron mass

Symbol: $m_n(x, y)$

Units: m_e

Identifier: [ELECTRON_MASS]

Functional dependence: POLY,VEGARD

Temperature dependence: ISOTHERMAL

7.4.8 Relative effective hole masses

7.4.8.1 Light hole mass

Symbol: $m_{lh}(x, y)$

Units: m_e

Identifier: [LIGHT_HOLE_MASS]

Functional dependence: POLY,VEGARD

Temperature dependence: ISOTHERMAL

7.4.8.2 Perpendicular light hole mass

Symbol: $m_{lh}(x, y)$

Units: m_e

Identifier: [LIGHT_HOLE_MASS_PERP]

Functional dependence: POLY,VEGARD

Temperature dependence: ISOTHERMAL

7.4.8.3 Parallel light hole mass

Symbol: $m_{lh}(x, y)$

Units: m_e

Identifier: [LIGHT_HOLE_MASS_PARA]

Functional dependence: POLY,VEGARD

Temperature dependence: ISOTHERMAL

7.4.8.4 Heavy hole mass

Symbol: $m_{hh}(x, y)$

Units: m_e

Identifier: [HEAVY_HOLE_MASS]

Functional dependence: POLY,VEGARD

Temperature dependence: ISOTHERMAL

7.4.8.5 Perpendicular heavy hole mass

Symbol: $m_{hh}(x, y)$

Units: m_e

Identifier: [HEAVY_HOLE_MASS_PERP]

Functional dependence: POLY,VEGARD

Temperature dependence: ISOTHERMAL

7.4.8.6 Parallel heavy hole mass

Symbol: $m_{hh}(x, y)$

Units: m_e

Identifier: [HEAVY_HOLE_MASS_PARA]

Functional dependence: POLY,VEGARD

Temperature dependence: ISOTHERMAL

When there is strain in the material, the effective masses of the light hole and the heavy hole are anisotropic. In this case, you can specify the perpendicular (to the heterojunction interface) and the parallel (to the heterojunction interface) effective masses separately in the material file. Harold will use the perpendicular effective masses to the calculation of confinement states in the quantum wells and the parallel effective masses to the carrier density calculation.

7.4.9 Minimum electron mobility

Symbol: $\mu_{1n}(x, y)$

Units: $cm^2 s^{-1} V^{-1}$

Identifier: [MIN_ELECTRON_MOBILITY]

Functional dependence: POLY

Temperature dependence: ISOTHERMAL

Comments: only relevant if 'DOPING' is used for the electron mobility.

7.4.10 Maximum electron mobility

Symbol: $\mu_{2n}(x, y)$

Units: $cm^2 s^{-1} V^{-1}$

Identifier: [MAX_ELECTRON_MOBILITY]

Functional dependence: POLY

Temperature dependence: ISOTHERMAL

Comments: only relevant if 'DOPING' is used for the electron mobility.

7.4.11 Electron mobility

Symbol: $\mu_n(x, y)$

Units: $cm^2 s^{-1} V^{-1}$

Identifier: [ELECTRON_MOBILITY]

Functional dependence: POLY, DOPING

Temperature dependence: THERMAL

7.4.12 Minimum hole mobility

Symbol: $\mu_{1p}(x, y)$

Units: $cm^2 s^{-1} V^{-1}$

Identifier: [MIN_HOLE_MOBILITY]

Functional dependence: POLY

Temperature dependence: ISOTHERMAL

Comments: only relevant if 'DOPING' is used for the hole mobility.

7.4.13 Maximum hole mobility

Symbol: $\mu_{2p}(x, y)$

Units: $cm^2 s^{-1} V^{-1}$

Identifier: [MAX_HOLE_MOBILITY]

Functional dependence: POLY

Temperature dependence: ISOTHERMAL

Comments: only relevant if 'DOPING' is used for the hole mobility.

7.4.14 Hole mobility

Symbol: $\mu_p(x, y)$

Units: $cm^2 s^{-1} V^{-1}$

Identifier: [HOLE_MOBILITY]

Functional dependence: POLY, DOPING

Temperature dependence: THERMAL

7.4.15 Electron Auger coefficient

Symbol: $C_n(x, y)$

Units: $cm^6 s^{-1}$

Identifier: [ELECTRON_AUGER]

Functional dependence: POLY

Temperature dependence: THERMAL

7.4.16 Hole Auger coefficient

Symbol: $C_p(x, y)$

Units: $cm^6 s^{-1}$

Identifier: [HOLE_AUGER]

Functional dependence: POLY

Temperature dependence: THERMAL

7.4.17 Electron free carrier absorption coefficient

Symbol: $\alpha_{fn}^0(x, y) = \alpha_{fw}^n(x, y)$

Units: cm^2

Identifier: [ELECTRON_FCA]

Functional dependence: POLY

Temperature dependence: ISOTHERMAL

7.4.18 Electron free carrier absorption coefficient

Symbol: $\alpha_{fp}^0(x, y) = \alpha_{fw}^p(x, y)$

Units: cm^2

Identifier: [HOLE_FCA]

Functional dependence: POLY

Temperature dependence: ISOTHERMAL

7.4.19 Spin-orbit splitting

Symbol: $E_{so}(x, y)$

Units: eV

Identifier: [SPIN_ORBIT_SPLIT]

Functional dependence: POLY

Temperature dependence: ISOTHERMAL

7.4.20 Lattice constant

Symbol: $a(x, y)$

Units: $Angstrom$

Identifier: [LATTICE_CONSTANT]

Functional dependence: VEGARD

Temperature dependence: ISOTHERMAL

For the lattice constant, an additional line must be added to the VEGARD function terms definitions: the first term of this line should specify the substrate lattice constant that the material is grown on. This is required for stress calculation of strain layer when the substrate and the layer material kinds are different. For example an AlGaInAs layer grown on InP layer. In this case, we can't deduce the lattice constant of InP from the material of AlGaInAs, so the InP lattice constant must be specified in the lattice constant section of the AlGaInAs material file.

7.4.21 Valence band strain-induced energy shift (hydrostatic)

Symbol: $E_{v.av}^{hy}(x, y)$

Units: eV

Identifier: [STRAIN_EVHY]

Functional dependence: POLY

Temperature dependence: ISOTHERMAL

Comments: The result of the polynomial evaluation is further multiplied by the normalized lattice mismatch $\Delta a(x, y)/a(x, y)$ where $\Delta a(x, y) = a_0 - a(x, y)$.

7.4.22 Conduction band strain-induced energy shift (hydrostatic)

Symbol: $E_c^{hy}(x, y)$

Units: eV

Identifier: [STRAIN_ECHY]

Functional dependence: POLY

Temperature dependence: ISOTHERMAL

Comments: The result of the polynomial evaluation is further multiplied by the normalized lattice mismatch $\Delta a(x, y)/a(x, y)$ where $\Delta a(x, y) = a_0 - a(x, y)$.

7.4.23 Strain-induced shear contribution to energy gap

Symbol: $\delta E^{sh}(x, y)$

Units: eV

Identifier: [STRAIN_ESH]

Functional dependence: POLY

Temperature dependence: ISOTHERMAL

Comments: The result of the polynomial evaluation is further multiplied by the normalized lattice mismatch $\Delta a(x, y)/a(x, y)$ where $\Delta a(x, y) = a_0 - a(x, y)$.

7.4.24 Bulk radiative constant

Symbol: B

Units: $cm^{-9}s^{-1}$

Identifier: [RADIATIVE_CONSTANT]

Comment: constant function

7.4.25 Band gap narrowing in QW regions

Symbol: $\Delta E_0^{(qw)}$

Units: $eVcm^{-1}$

Identifier: [GAP_NARROWING_QW]

Comment: constant function

7.4.26 Donor-induced band gap narrowing in bulk regions

Symbol: $\Delta E_0^{(n)}$

Units: $eVcm^{-1}$

Units: $cm^{-9}s^{-1}$

Identifier: [GAP_NARROWING_N]

Comment: constant function

7.4.27 Acceptor-induced band gap narrowing in bulk region

Symbol: $\Delta E_0^{(p)}$

Units: $eVcm^{-1}$

Units: $cm^{-9}s^{-1}$

Identifier: [GAP_NARROWING_P]

Comment: constant function

7.4.28 Usage Conditions of the material

Identifer: [STRAINED_LAYER]

Comment: 1 means the material can be used for a strained layer; 0 means it can not be used for a strained layer

7.5 Thermal models

Temperature dependence has been included for the following material parameters:

7.5.1 Gap

$$E_g\left(x,y,T\right)=E_g\left(x,y\right)+a\left(\frac{T^2}{T+e}-\frac{T_0^2}{T_0+e}\right)$$

Syntax:

'*THERMAL*'

3,

$a,e,T_0,$

7.5.2 Electron Affinity

$$\chi(x, y, T) = \chi(x, y) + a\left(\frac{T^2}{T+e} - \frac{T_0^2}{T_0+e}\right)$$

Syntax:

'*THERMAL*'

3,

$a, e, T_0,$

7.5.3 Refractive index

$$\overline{n}(x, y, T) = \overline{n}(x, y) + d(T - T_0)$$

Syntax:

'*THERMAL*'

2,

$d, T_0,$

7.5.4 Thermal resistivity

$$\rho_{th}(x, y, T) = \rho_{th}(x, y)\left(\frac{T}{T_0}\right)^d$$

Syntax:

'*THERMAL*'

2,

$d, T_0,$

7.5.5 Auger coefficients

$$C_{n,p}(x, y, T) = C_{n,p}(x, y)\exp\left[T_a\left(\frac{1}{T} - \frac{1}{T_0}\right)\right] \times \begin{cases} 1 & bulk \\ \sqrt{\dfrac{T}{T_a}} & quantum \quad well \end{cases}$$

Syntax:

'*THERMAL*'

2,

$Ta, T_0,$

7.5.6 Mobility

If the functional dependence is " POLY", then

$$\mu = \mu_0\left(\frac{T}{T_0}\right)^{d_1}$$

where μ_0 is calculated by the "POLY" function.

Syntax:

      '*THERMAL*'

      2,

      $d_1, T_0,$

If the functional dependence is "DOPING", then

$$\mu = \mu_1 \left(\frac{T}{T_0} \right)^{d_1} + \frac{(\mu_2 - \mu_1) \left(\dfrac{T}{T_0} \right)^{d_2}}{\left(1 + \left[\dfrac{N_D + N_A}{N_r \left(\dfrac{T}{T_0} \right)^{d_3}} \right] \right)^{\alpha}}$$

where μ_1 and μ_2 is the minimum and maximum mobility respectively.

Syntax:

      '*THERMAL*'

      4,

      $d_1, d_2, d_3, T_0,$

Chapter

8

Numerical Implementation

HAROLD attempts to solve eqs. (3-1) through (3-6) in a discrete one-dimensional mesh. In other words, the differential equations are first discretised and transformed into a set of *non-linear algebraic* equations, using finite differences. In order to find an *approximate* numerical solution of the set of discretised equations, HAROLD employs an iterative scheme based on the well-known Newton-Raphson method. The accuracy of the obtained solution depends, essentially, on the following factors:

- Choice of the mesh

- Injection level

- Numerical precision

This Chapter discusses how to control the evolution of the simulation, so that a 'good solution' of the set of equations for a particular device can be achieved.

8.1   Program structure

Before to discuss the numerical procedures it is instructive understand first how the program has been structured, from a global point of view. **Figure 8.1** shows the flow diagram of HAROLD.

Right after startup, HAROLD reads the input, sets the working mesh and assigns to every point the necessary parameters. It then solves the waveguide equation (3-50) to determine the profile of the optical mode, and the Schrödinger's equation to figure out the quantum well levels (or read them from a definition file). Note that both optical mode and quantum well levels are assumed to remain unchanged throughout the simulation, i.e., they are not solved self-consistently with the device and optical equations.
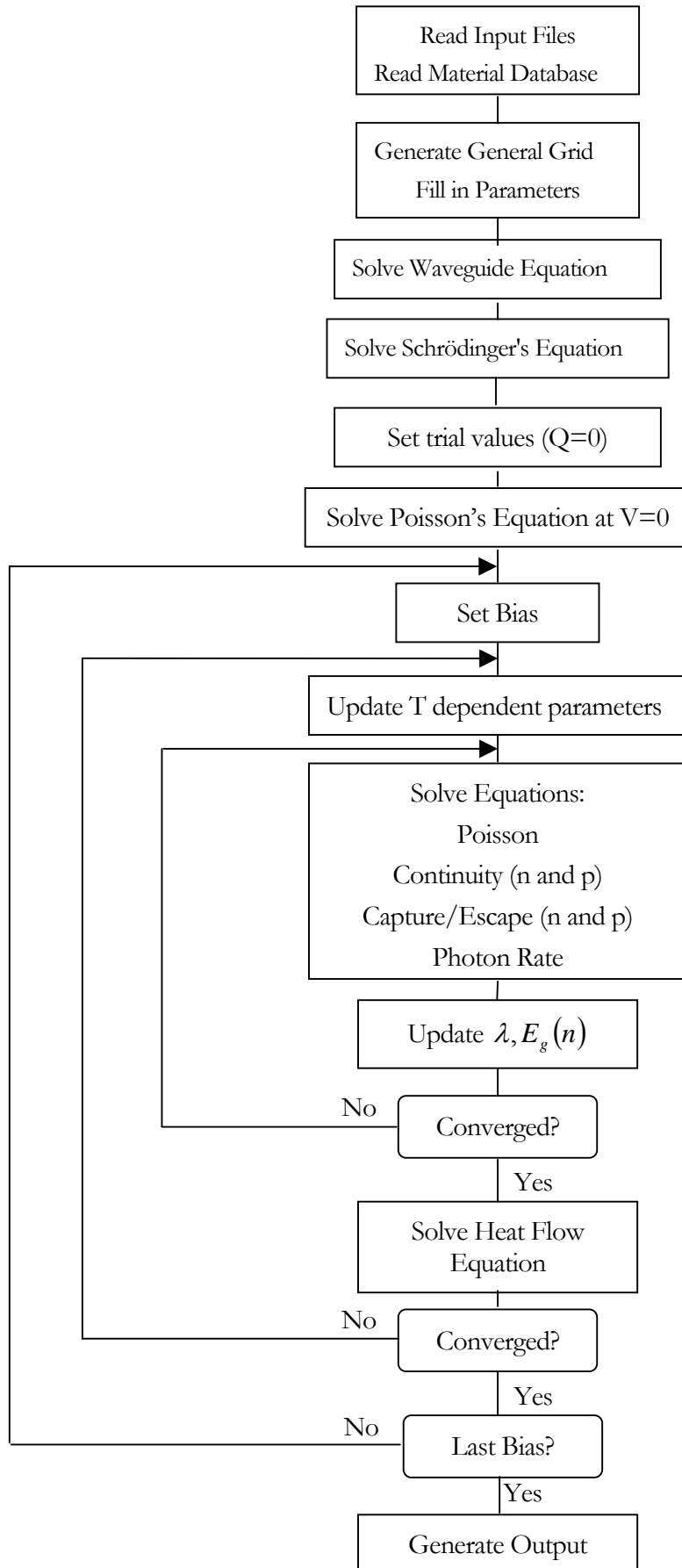
Figure 8.1: HAROLD's flow chart

In its quest for seeking the solution for a given bias level, HAROLD employs an iterative scheme based on the Newton-Raphson algorithm. One of the essential points for the applicability of the Newton-Raphson method is to know *a priori* a first approximation to the solution of the system of equations, in other words, to have an initial guess. This is achieved at the beginning of the simulation by solving Poisson's equation only, at zero voltage. The outcome constitutes the initial guess for the first bias level. For the subsequent bias, the initial guess is always the solution at the previous bias.

At each bias (either voltage or current controlled) the flow stream is the following.

First, HAROLD seeks a solution of the electric and optical equations, assuming a fixed temperature field. The solution is further refined to account for bandgap narrowing and wavelength shift effects. Once a stable solution has been found, the program proceeds to evaluate the new temperature distribution by means of solving the heat flow equation. With this new temperature distribution, the temperature dependent parameters are updated and the electric equations again solved to reflect the changes in temperature. The entire cycle is repeated until consistency between thermal and electrical solutions is achieved.

The execution of the program continues until the last bias is reached.

8.2   Residuals

In order to control the accuracy of the solution it is convenient to introduce the concept of *residual* of an equation. Once the device equations have been conveniently discretised, by means of applying the method of finite differences, one obtains a set of six functions F_k of the independent variables evaluated at discrete points y_i, $i = 1, ..., NY$, where NY is the total number of nodes in the mesh. For a given set of values of the independent variables, the values of the F_k's are the *residuals*. The solution of the system corresponds to that set of values of the independent variables for which all F_k vanish identically. Obviously, this cannot be achieved in practice, so the most we can do is to try to make the residuals as small as possible.

In order to make the previous definition of the residuals a useful one, the differential equations have been scaled. This is achieved by means of multiplying them by appropriate factors in such a way that the resulting residuals become dimensionless quantities. The scaling factors used for the fundamental quantities are shown in **Table 8.1**. This particular choice of the scaling allows one to take the residuals as a direct measure of the accuracy of the actual computation.

Quantity	Scaling factor
y	L_y
ϕ	kT_0 / q
n, p, N_A, N_D	$\max(N_A(y), N_D(y)), \quad 0 \le y \le L_y$
D_n, D_p	$\max(D_n(y), D_p(y)), \quad 0 \le y \le L_y$

Table 8.1: Scaling factors used in the simulation.

8.3 Iterative scheme

As we have seen, HAROLD employs an iterative scheme based on the Newton-Raphson algorithm to obtain the solution of the electrical and optical equations. This means that, for each iteration cycle, HAROLD calculates a correction $\delta\phi^{(k)}$ to the previous values of the potentials, which are then updated according to

$$\phi^{(k+1)} = \phi^{(k)} + \frac{\delta\phi^{(k)}}{1 + \left| \delta\phi^{(k)} / \delta\phi_{clamp} \right|}$$

where $\delta\phi_{clamp}$ is a clamp potential introduced to prevent the breakdown of the method in some critical situations.

In addition, we define a normalized correction as

$$\delta\widetilde{\phi}^{(k)} = \left| \frac{\delta\phi^{(k)}}{\phi^{(k+1)}} \right|$$

which, in turn, constitutes a measure of the numerical accuracy.

The iterative scheme is assumed to converge whenever at least one of the following criteria applies:

1. All residuals of the equations are smaller than a predefined limit
2. All normalized corrections are smaller than a predefined limit

The first criterion implies that the values of the potentials (i.e. the solution) that HAROLD obtained constitute, in fact, a solution of the *discretised* differential equations, within the required error. The second criterion serves to stop the Newton-Raphson method whenever a *stable* solution has been reached. Note that a *stable* solution does not necessarily imply a *good* solution.

8.4 Control of the simulation

HAROLD allows the user to control the accuracy of the solution by specifying the following parameters:

* Upper limit for the residuals

  Maximum value any residual can take. If all residuals are smaller than this value the iteration will stop.

* Upper limit for the normalized corrections (numerical accuracy)

  Maximum value any normalized correction can take. If all normalized corrections are smaller than this value the iteration will stop.

* Maximum number of iterations

  When to stop if both of the above criteria fail.

* Clamping value of the potentials

  On the average, the maximum value that the potentials are allowed to change from one iteration step to another.

- Temperature resolution

  Accuracy of the temperature distribution.

- Wavelength resolution

  Accuracy of the lasing wavelength.

Convergence to the required accuracy at a given bias can fail if the bias step (voltage or current step) is too large, as the solution at the previous might then constitute a poor initial guess solution for the present bias. This can be prevented by reducing the voltage increment and/or current step, or by enabling the adaptiveBiasStep feature which will automatically reduce the bias step size when needed.

You can set these parameters in the *Simulator* panel (see Section 5.3). HAROLD provides default values for the numerical parameters, which are adequate for most laser structures biased above 1 Volt.

Chapter

9

Command-Line and Client/Server Interface

Please refer to the Scripting Manual for HAROLD (Harold\Documents\ScriptingManual.pdf on your CD).

Appendix A

Glossary of symbols

Here we present the description of symbols appearing in this manual. The sources of the input values used for quantities that are external to the program are indicated next their respective symbols.

A_{ji}^{pol}	Anisotropy factor for the dipole moment.
B	Radiative recombination constant [Database].
b_m	Total losses, defined as $\alpha_m + \alpha_{int}$.
C_n, C_p	Auger recombination coefficients for electrons (n) and holes(p) [Database].
c	Velocity of light in vacuum.
d_w	Width of the quantum well [Device file].
E	Photon energy.
E_g	Band gap [Database].
E_j^0, E_i^0	Energy levels of the j-th and i-th states in a quantum well, relative to the bottom of the well. The j refers to the conduction band levels, while i refers to the valence band and sub-band levels.
E_{ij}	Energy difference between the j-th and i-th levels.
E_{fn}, E_{fp}	Quasi-Fermi energies for unconfined electrons (n) and holes (p), defined as $-q\phi_n$ and $-q\phi_p$, respectively.
E_{fn}^w, E_{fp}^w	Quasi-Fermi energies for confined electrons (n)and holes (p).
E_k	Energy level of the k-th deep trap .
f_j, f_i	Fermi occupation factors for the j-th and i-th levels.
g_m	Interband modal gain.
g	Interband local gain.
G	Broadened gain.
$\hbar$	Planck's constant divided by 2π.
j_n, j_p	Current densities for electrons (n) and holes (p).
j_{ext}	Externally injected current density [User].
k_0	Wave vector in vacuum at peak mode gain.

k	Boltzmann constant.
L	Device transverse length.
$L(\ )$	Lorentzian line shape function.
L_{cav}	Laser cavity length (User).
m_e	Mass of the electron.
m_n'	Corrected electron effective mass [Advanced User].
m_j, m_i	Effective masses of the j-th and i-th levels.
m_{ij}	Reduced effective mass.
m_n, m_p	Bulk effective masses for electrons and holes [Database].
M_0	Momentum matrix element.
N_c, N_v	Density of states of the conduction (c) and valence (v) bands.
N	Total number of nodes .
N_D, N_A	Doping density of donors (D) and acceptors (A) .
N_k	Density of the k-th trap .
n	Density of unconfined (3D) electrons.
n_i, n_r	Intrinsic carrier density and its value for the reference material.
n_j	Density of confined (2D) electrons for the j-th level.
n_w	Total density of confined electrons.
n_{ij}	Intrinsic carrier density associated to the j-th and i-th levels.
$\bar{n}$	Real part of the refractive index [Database].
n_{eff}	Effective refractive index.
p	Density of unconfined (3D) holes.
p_i	Density of confined (2D) holes for the i-th level.
p_w	Total density of confined (2D) holes.
q	Charge of the electron.
R^{SRH}	Shockley-Read-Hall recombination rate per unit volume (bulk).
R^{Spont}	Spontaneous recombination rate per unit volume (bulk).
R^{Auger}	Auger recombination rate per unit volume (bulk).
R_n^{net}, R_p^{net}	Net recombination rate per unit volume, for electrons (n) and holes (p).

r_{sp}, R_{qw}^{Spont}	Energy (frequency) dependent spontaneous recombination rate per unit volume , for confined carriers.
R^{Stim}	Stimulated recombination rate per unit volume.
$r_m^{(1)}, r_m^{(2)}$	Reflectivities for facet 1 and 2 [User].
s_m	Single facet scattering loss coefficient [User].
$\langle S \rangle$	Average density of photons in the cavity.
T	Temperature [User].
T_0	Room temperature [300 K].
V_{ext}	Voltage bias [User].
v	Volume of the cavity.
$\langle v_n \rangle, \langle v_p \rangle$	Average thermal velocity of electrons (n) and holes (p).
W	Optical wave function.
x, y, z	Spatial coordinates used in the model. x and y are the directions parallel and perpendicular to the to the active layer, respectively, while z is the direction of light emission.
α_m	Facet loss coefficient, defined as $L^{-1} \log\left(1/\sqrt{r_m^{(1)} r_m^{(2)}}\right)$.
α_{int}	Internal scattering loss coefficient [User].
$\alpha_{fn}^0, \alpha_{fp}^0$	Free carrier absorption rate for unconfined electrons (n) and holes (p) [Database].
$\alpha_{fw}^n, \alpha_{fw}^p$	Free carrier absorption rate for confined electrons (n) and holes(p) [Database].
β	Fraction of spontaneous emission that couples to the lasing mode[Advanced User].
ε	Complex optical dielectric constant.
ε_d	Relative dielectric constant [Database].
ε_0	Dielectric constant of vacuum.
ΔE_{g0}	Bandgap shrinkage coefficient.
γ	Half width of the Lorentzian broadening function.
γ_{sp}	Spontaneous recombination correction factor, =**sponRecombFac** in interface [Advanced User].
λ	Optical wavelength.
μ_n, μ_p	Mobility of electrons (n) and holes (p) [Database].
ρ_j, ρ_i	Density of states for the j-th and i-th levels (e.g., $\rho_i = m_i / \pi \hbar^2 d_w$).

ρ_{ij}	Reduced density of states for the transition between the j-th and i-th levels.
ϕ	Electrostatic potential.
ϕ_b	Built-in potential.
ϕ_n, ϕ_p	Quasi-Fermi potentials for unconfined electrons (n) and holes(p).
ϕ_{nw}, ϕ_{pw}	Quasi-Fermi potentials for confined electrons (n) and holes (p).
θ_n, θ_p	Band edge for unconfined electrons (n) and holes (p).
θ_{nw}, θ_{pw}	Band edge for confined electrons (n) and holes (p).
$\sigma_{nk}^0, \sigma_{pk}^0$	Electron (n) and hole (p) capture cross section of the k-th deep trap, at T_0 [deep trap definition file].
τ_{in}	Intraband scattering lifetime [Advanced User].
τ_{n0}, τ_{p0}	Effective electron (n) and hole (p) SRH lifetimes [Database /Advanced User].
$\tau_n^{cap}, \tau_p^{cap}$	Electron (n) and hole (p) capture time [Advanced User].
τ_{nk}, τ_{pk}	Electron (n) and hole (p) lifetimes due the k-th deep trap
χ, χ_r	Affinity, and that of the reference material [Database].
υ_g	Group velocity.
ω	Angular frequency of the optical wave.

Appendix B

Bibliography

DIODE LASERS AND PHOTONIC INTERGRATED CIRCUITS
L.A. Coldren and S.W. Corzine
John Wiley & Sons, New York, 1995, ISBN 0-471-11875-3.

QUANTUM WELL LASERS
Edited by Peter S. Zory, Jr.
Academic Press, San Diego, 1993, ISBN 0-12-781890.

ANALYSIS AND SIMULATION OF SEMICONDUCTOR DEVICES
S. Selberherr
Springer Verlag, Wien, 1984, ISBN 3-211-81800-6.

TWO-DIMENSIONAL MODELING OF QUANTUM-WELL SEMICONDUCTOR LASERS
Z.M. Li, K.M. Dzurko, and S.P. McAlister
International Journal for Computation and Mathematics in Electrical and Electronic Engineering, Vol. 10, No. 4, p. 225, James Science Publishers Ltd.

A SELF-CONSISTENT TWO-DIMENSIONAL MODEL OF QAUNTUM WELL SEMICONDUCTOR LASERS: OPTIMIZATION OF A GRIN-SCH SQW LASER STRUCTURE
Z.M. Li, K.M. Dzurko, A. Deland S.P. McAlister
IEEE J. Quantum Electron. , Vol. 28, 1992, p.792.

TWO-DIMENSIONAL NONISOTHERMAL FINITE ELEMENT SIMULATION OF LASER DIODES
Gen-Lin Tan, N. Bewtra, K. Lee, and J.M. Xu
IEEE J. Quantum Electron., Vol. 29, No. 3, 1993. p. 822.

TWO-DIMENSIONAL SIMULATION OF CONSTRICTED-MESA INGAASP/INP BURIED-HETEROSTRUCTURE LASERS
M. Gault, P. Mawby, A. R. Adams, and M. Towers
IEEE J. Quantum Electron., Vol. 30, No. 8, 1994, p. 1691.

A MODEL FOR GRIN-SCH-SQW DIODE LASERS
S.R. Chin, P.S. Zory, and A.R. Reisinger
IEEE J. Quantum Electron., vol. QE23, 1988, p. 2191.

CARRIER ESCAPE TIME IN GAAS/ALGAAS AND INGAAS/GAAS QUANTUM-WELL LASERS

Esquivias, B. Romero, S. Weisser, K. Czotscher, J.D. Ralston,E. C. Larkins, J.Arias,

A. Schönfelder, M. Mikulla, J. Fleissner,and J. Rosenzweig

Proceedings from the SPIE Conference, vol. 2694, 1996, pp. 17-25.

CORRECTIONS TO THE EXPRESSION FOR GAIN IN GAAS

R.H. Yan, S.W. Corzine, L.A.Coldren, and I. Suemune

IEEE J. Quantum Electron., Vol. 26, No. 2, 1990. p. 213.

SELF-HEATING EFFECTS IN BASIC SEMICONDUCTOR STRUCTURES

A. Amerasekera, Mi-Chang Chang, J.A. Seitchik, A. Chatterjee, K. Mayaram, and Jue-Hsien Chern

IEEE Trans. Electron. Devices Vol. 40, No. 10, 1993, p. 1836.

RIGOROUS THERMODYNAMIC TRATMENT OF HEAT GENERATION AND CONDUCTION IN SEMICONDUCTOR DEVICE MODELING

G. K. Wachutka

IEEE Trans. Comput-Aided Des. Integrat. Circuits Syst., Vol. 9, 1990,p. 1141.

PROPERTIES OF ALUMINIUM GALLIUM ARSENIDE

Edited by S. Adachi

Guma University, IEE Inspec.

GAAS, ALAS, ALXGA1-XAS: MATERIAL PARAMETERS FOR USE IN RESEARCH AND APPLICATIONS

S.Adachi

J. Appl. Phys., Vol. 58, 1985, R1.

LATTICE THERMAL RESISTIVITY OF III-V COMPOUND ALLOYS

S. Adachi

J. Appl. Phys., Vol. 54, 1983, p. 1844.

Index